Atmos. Chem. Phys. Discuss., 13, 8153–8211, 2013
www.atmos-chem-phys-discuss.net/13/8153/2013/
doi:10.5194/acpd-13-8153-2013

Atmospheric Chemistry and Physics Discussions

Tethered balloon-borne aerosol measurements: seasonal and vertical variations of aerosol constituents over Syowa Station, Antarctica

K. Hara[1,*], **K. Osada**[2], **and T. Yamanouchi**[1]

[1]National Institute of Polar Research, Tokyo, Japan
[2]Graduate School of Environmental Studies, Nagoya University, Nagoya, Japan
[*]now at: Department of Earth System Science, Faculty of Science, Fukuoka University, Fukuoka, Japan

Received: 15 January 2013 – Accepted: 12 March 2013 – Published: 26 March 2013

Correspondence to: K. Hara (harakei@fukuoka-u.ac.jp)

Published by Copernicus Publications on behalf of the European Geosciences Union.

Abstract

Tethered balloon-borne aerosol measurements were conducted at Syowa Station, Antarctica during the 46th Japanese Antarctic expedition (2005–2006). Direct aerosol sampling was operated from near the surface to the lower free troposphere (approximately 2500 m) using a balloon-borne aerosol impactor. Individual aerosol particles were analyzed using a scanning electron microscope equipped with an energy dispersive X-ray spectrometer. Seasonal and vertical features of aerosol constituents and their mixing states were investigated. Results show that sulfate particles were dominant in the boundary layer and lower free troposphere in the summer, whereas sea-salt particles were dominant during winter–spring. Minerals, $MgSO_4$, and sulfate containing K were identified as minor aerosol constituents in both boundary layer and free troposphere over Syowa Station. Although sea-salt particles were dominant during winter–spring, the relative abundance of sulfate particles increased in the boundary layer when air masses fell from the free troposphere over the Antarctic coast and continent. Sea-salt particles were modified considerably through heterogeneous reactions with SO_4^{2-}, $CH_3SO_3^-$, and their precursors during the summer, and were modified slightly through heterogeneous reactions with NO_3^- and its precursors. During winter–spring, sea-salt modification was insignificant, particularly in the cases of high relative abundance of sea-salt particles and higher number concentrations. In August, NO_3^- and its precursors contributed greatly to sea-salt modification over Syowa Station. Because of the occurrence of sea-salt fractionation on sea-ice, Mg-rich sea-salt particles were identified during April–November. In contrast, Mg-free sea-salt particles and slightly Mg-rich sea-salt particles co-existed in the lower troposphere during summer. Thereby, Mg separation can proceed by sea-salt fractionation during summer in Antarctic regions.

ACPD
13, 8153–8211, 2013

1 Introduction

Atmospheric aerosol measurements have been made in Antarctic regions for several decades from numerous perspectives, for instance, atmospheric material cycles, monitoring of Earth background levels, radiation budgets, and ice core record interpretation (e.g. Shaw, 1988; Ito, 1989; Legrand and Mayewski, 1997; Bromwich et al., 2012). Because of restrictions on logistics under severe conditions, most investigations of aerosol constituents were conducted at coastal stations such as Syowa Station, Neumayer Station, Halley Station, Dumont d'Urville Station, Mawson Station, and Aboa Station (e.g. Savoie et al., 1992, 1993; Teinilä et al., 2000; Legrand et al., 2001; Hara et al., 2004; Weller et al., 2011). Recently, aerosol measurements have been taken even at inland stations such as Amundsen–Scott (South Pole) Station, Dome F Station, Kohnen Station, and Concordia (Dome C) Station (e.g. Bodhaine, 1995; Hara et al., 2004; Jourdain et al., 2006; Weller et al., 2007; Udisti et al., 2012).

Major aerosol constituents are SO_4^{2-}, $CH_3SO_3^-$, NO_3^- sea-salts (e.g. Na^+ and Cl^-) in the Antarctic troposphere. Minor aerosol constituents are minerals and carbonaceous species (soot and organics). Particularly, SO_4^{2-} and $CH_3SO_3^-$ are strongly dominant during the summer (e.g. Minikin et al., 1998; Legrand et al., 2001). Size segregated aerosol analysis showed that SO_4^{2-} and $CH_3SO_3^-$ were distributed mainly in the submicrometer range at the Antarctic coasts (e.g. Jourdain and Legrand, 2001; Read et al., 2008). Although the concentrations of SO_4^{2-} and $CH_3SO_3^-$ reached maximum values in the summer because of biogenic activity in the ocean (e.g. Minikin et al., 1998), high amounts of SO_4^{2-} and$CH_3SO_3^-$ were found during winter–spring at coastal stations (Minikin et al., 1998; Jourdain and Legrand, 2001; Preunkert et al., 2008; Read et al., 2008). In contrast to strong summer maxima of SO_4^{2-} and $CH_3SO_3^-$ in aerosols (Minikin et al., 1998; Jourdain and Legrand, 2001; Preunkert et al., 2008; Read et al., 2008), the high concentrations of DMS and DMSO remained in winter at coastal and continental stations because of their longer lifetime by weak photochemical processes during the winter (Jourdain and Legrand, 2001; Preunkert et al., 2008; Read et al.,

ACPD
13, 8153–8211, 2013

2008). Particularly high concentrations of DMS and DMSO found at inland stations during winter implied considerable poleward transport to the interior of the continent.

Sea-salts are dominant during winter–spring (e.g. Hara et al., 2004). Sea-salt particles were distributed widely in ultrafine-coarse mode throughout the year at Syowa Station (Hara et al., 2010a, 2011a) and were distributed in fine-coarse mode during the summer at Aboa Station (Kerminen et al., 2000; Teinilä et al., 2000). Sea-salt particles can play important roles as scavengers of acidic species and as the origin of reactive halogen species through heterogeneous reactions in the Antarctic troposphere (e.g. Hara et al., 2004). Single particle analysis using an electron microscope equipped with an energy dispersive X-ray spectrometer (SEM-EDX) suggested that sea-salt particles near the surface were modified with SO_4^{2-} and $CH_3SO_3^-$ during the summer, and were modified with NO_3^- in August at Syowa Station (Mouri et al., 1999; Hara et al., 2005). Results obtained using other microprobe techniques such as laser microprobe mass spectrometry have implied that SO_4^{2-} and $CH_3SO_3^-$ were mixed internally with sea-salt particles (Wouters et al., 1990; Hara et al., 1995). Furthermore, sea-salt particles in the free troposphere over Syowa Station were modified not only with SO_4^{2-} but also with NO_3^- during the summer (Hara et al., 2006). In addition to sea-salt modification, sea-salt particles were fractionated through precipitation of several salts such as mirabilite (Na_2SO_4 $10H_2O$) and hydrohalite (NaCl $2H_2O$) in sea ice formation under colder conditions (e.g. Wagenbach et al., 1998; Hara et al., 2004, 2012). Concomitantly with the expansion of sea-ice regions during winter–spring, the contributions of sea-salt particles derived from sea-ice and frost flower increased significantly (e.g. Wagenbach et al., 1998; Rankin et al., 2000, 2002; Hara et al., 2004, 2012). Fractionated sea-salt particles in coastal regions originate from sea-ice and frost flower (Wagenbach et al., 1998; Rankin et al., 2000, 2002; Hara et al., 2004, 2012). Therefore, sea-salt particles have been used as tracers (Hara et al., 2010a, 2011a) and as an index of sea-ice extent (e.g. Wolff et al., 2006).

Regarded from the viewpoint of transport processes and material cycles, measurements of aerosol constituents such as black carbon and radionuclides have been con-

ACPD
13, 8153–8211, 2013

ducted in Antarctic regions (Fiebig et al., 2009; Hara et al., 2010a; Elsässer et al., 2011). Continuous aerosol measurements at coastal stations suggest the substantial transport of combustion-origin aerosol particles from biomass burning in South America and southern Africa (Fiebig et al., 2009; Hara et al., 2010a,b). Our previous investigation (Hara et al., 2010a) revealed that long-range transport from biomass burning and mixing of sea-salt particles cause aerosol-enhanced (haze) conditions at Syowa Station. The variety of radionuclides (^{7}Be, ^{10}Be and ^{210}Pb) implied meridional transport to Antarctic coasts and mixing of stratospheric air into the troposphere (Elsässer et al., 2011). Previous investigations provided important knowledge about aerosol chemical properties near the surface, for example, concentrations, seasonal variations, and size distributions. Because of the dearth of knowledge of aerosol chemistry in the upper atmosphere, aerosol chemical properties and chemical processes have been discussed mainly on the basis of results obtained from aerosol measurements near the surface. Recent ground-based aerosol measurements have revealed atmospheric processes that take place in the upper atmosphere: (1) accumulation of DMS and DMSO in the free troposphere and buffer layer (Legrand et al., 2001; Preunkert et al., 2008); (2) aerosol transport into inland areas through the free troposphere (Piel et al., 2006); (3) high abundance of volatile particles (e.g. sulfate particles) in the free troposphere during the winter (Hara et al., 2011a); and (4) the likelihood of new particle formation (Koponen et al., 2003). Consequently, in-situ aerosol measurements in the upper atmosphere are necessary for better understanding of aerosol and other atmospheric processes in the Antarctic regions. Particularly direct aerosol sampling must be made in the upper atmosphere to elucidate atmospheric material cycles and atmospheric chemistry in the Antarctic troposphere.

Although airplanes, launched balloons and tethered balloons have been used to measure aerosols in the upper atmosphere in Antarctic regions (Iwasaka et al., 1985; Ito et al., 1986; Yamazaki et al., 1989; Yamanouchi et al., 1999; Hayashi, 2001; Wada et al., 2001; Rankin and Wolff, 2002; Hara et al., 2006, 2011b; Osada et al., 2006; Kizu et al., 2010), direct aerosol sampling in the upper atmosphere has been conducted

ACPD
13, 8153–8211, 2013

only for those aerosol measurements reported by Iwasaka et al. (1985), Yamazaki et al. (1989), Rankin and Wolff (2002), and Hara et al. (2006). These previous studies have revealed major aerosol constituents in the boundary layer and free troposphere and the likelihood of transport of sea-salt and mineral particles through the free troposphere. Tethered balloon-borne and airplane-borne aerosol measurements (Osada et al., 2006; Hara et al., 2011b) have shown high concentrations of condensation nuclei (CN, $D_p > 10$ nm) by new particle formation in the lower free troposphere over Syowa Station. Because of operational limitations, seasonal features of vertical distributions of aerosol constituents in the upper atmosphere have never been completely understood. In this study, tethered balloon-borne aerosol measurements were performed to elucidate the vertical and seasonal features of aerosol constituents and their mixing states in the Antarctic troposphere. Herein, we mainly discuss (1) seasonal and vertical distributions of aerosol constituents, (2) sea-salt chemistry, and (3) vertical structures of Antarctic haze.

2 Aerosol sampling and analysis

Tethered balloon operations were conducted at the C-heliport of Syowa Station, Antarctica (69° 00′ S, 39° 35′ E) on East Ongul Island, which is located in Lutzow Holm Bay and which lies ca. 4 km distant from the Prince Olav coast of Antarctic continent. The distance from Syowa Station to the sea-ice margin was approximately 100 km during the summer and 1000 km during winter–spring. The C-heliport (ca. 15 m a.s.l.) is located at the windward side of prevailing winds and ca. 600 m distant from the main area having a diesel power station. For safe operation, tethered-balloon-borne aerosol measurements were made under conditions with weaker surface winds (mean $< 5\,m\,s^{-1}$). In the case of strong winds ($> 12\,m\,s^{-1}$) in the upper atmosphere, the balloon stopped ascending and then descended to avoid breakage of the tether-line and balloon. When thick clouds appeared at observable altitudes over Syowa Station, the measurements stopped around the cloud base. In the case of thin clouds, aerosol measurements were

ACPD
13, 8153–8211, 2013

continued above the clouds. Aerosol measurements and sampling were operated in afternoon (LT) during January–April and September–December and at 10:45–15:30 (LT) during May–August because safe operation required visible identification of tethered balloon under light and dusk conditions.

A tethered-balloon system (Vaisala) was used to aerosol measurements to ascertain vertical features of aerosol number concentrations and aerosol constituents in the lower troposphere. Details of instruments for the tethered balloon-borne aerosol measurements were described by Hara et al. (2011b). Figure 1 depicts an example of the balloon trajectory during aerosol measurements. Measurements using a condensation particle counter (CPC), an optical particle counter (OPC), and aerosol sampling were conducted independently because of payload limitations. During the first flight, the aerosol number concentration and meteorological parameters were measured using CPC, OPC, and tether-sonde. Second, direct aerosol sampling was conducted using an aerosol impactor and tether-sonde.

A two-stage aerosol impactor developed by Okada et al. (1997) was customized by removal of the timer system and by addition of a radio-control system for the tethered balloon-borne aerosol sampling conducted for this study. The cut-off diameter of the impactor was 0.2 µm and 2.0 µm at a flow rate of 1.2 L min^{-1}. During the second flight, aerosol samples taken at 3–5 levels (depending on the highest altitude of the first flight) were chosen based on vertical profiles of air temperature and relative humidity. The altitude was maintained during aerosol sampling. Each aerosol sampling required 10–15 min, as shown in Fig. 1. The aerosol impactor was controlled manually by radio commands from the ground. Aerosol particles were collected on the carbon-coated collodion thin film supported by Ni-TEM grid. Unfortunately, aerosol samples were not taken on 6 January, 15 January, or 1 August because of mechanical trouble that occurred with the impactor and the tethered balloon system.

After aerosol measurements/sampling, aerosol samples were kept in polyethylene capsules. To avoid contamination, aerosol samples were handled under clean air flow of a clean-bench. The polyethylene capsules with aerosol samples were packed into

ACPD
13, 8153–8211, 2013

polyethylene bags with a zipper. All bags with aerosol samples were put into an airtight box together with a desiccant (NISSO-DRY M; Nisso Jushi Co. Ltd.) until analysis to prevent humidification that can engender morphology change and efficient chemical reactions. We used SEM-EDX (Quanta FEG-200F; FEI Co., and XL30; EDAX Inc.) for elemental analyses of single particles. To avoid analytical bias of localization of aerosol constituents in each particle, the rectangular or square area almost covering a particle was scanned using an electron beam in EDX analysis. Procedures and conditions of single-particle analysis were in accordance with those described by Hara et al. (2002, 2005). We analyzed 37 533 particles in fine mode (D_p: 0.2–2.0 µm) and 2095 particles in coarse mode (D_p > 2.0 µm) in this study. Because of the lower number density, none to several particles were analyzed in some samples in coarse mode.

3 Results and discussion

3.1 Meteorological conditions during aerosol sampling

Figure 2 depicts vertical profiles of potential temperature and relative humidity in the direct sampling flight. A surface inversion layer was identified in many cases (particularly during winter–spring). The surface inversion layer height was < 100 to ca. 350 m. The altitude of the boundary layer top was approximately 500–1200 m, as inferred from comparison of vertical features of potential temperature, relative humidity, and aerosol number density (Hara et al., 2011a). As shown in Fig. 2, direct aerosol sampling was conducted in the surface inversion layer, boundary layer, and free troposphere. Unfortunately, few aerosol samples were taken at the highest altitudes (> 1400 m) during May–August because of radio communication trouble.

3.2 Backward trajectory from the sampling altitudes

Figure 3 depicts typical examples of 5-day backward trajectory from the altitudes of aerosol sampling over Syowa Station. The trajectory was computed using vertical mo-

ACPD
13, 8153–8211, 2013

tion mode in the NOAA-HYSPLIT model with the "NCEP reanalysis" dataset (Draxler and Rolph, 2013). The air mass history in this study was classified into four types, as shown in Fig. 3. On 26 January (Fig. 3a), air masses were transported westward along the coastline. According to Suzuki et al. (2004), this pathway was dominant at Syowa Station during the summer. On 5 March (Fig. 3b), air masses in the boundary layer came from the free troposphere over the interior of the continent. Furthermore, air masses were transported downward along the continental surface. This transport path might result from effects of katabatic wind. In contrast, air masses in the free troposphere came eastward from the free troposphere over the coast and Southern Ocean. On 28 May (Fig. 3c), air masses in the boundary layer and free troposphere were transported from the Southern Ocean. In addition, air parcels were lifted from the boundary layer to the free troposphere. This flow pattern was associated with the approach of a cyclone, as explained by Hara et al. (2010a). On 16 June (Fig. 3d), air masses in the boundary layer were transported from the interior of the continent, similar to the case on 5 March, whereas air masses in the free troposphere came from the Southern Ocean. This transport pathway was consistent with vertical features of potential temperature and relative humidity (Fig. 2). All backward trajectories are presented in Supplement.

3.3 Aerosol constituents collected in the lower troposphere over Syowa Station

Figure 4 presents typical examples of SEM images of aerosol particles collected in the tethered-balloon-borne aerosol sampling. Most aerosol particles exhibited the satellite structure shown in Fig. 4a. This unique morphology was observed predominantly in the Antarctic troposphere (Yamato et al., 1987; Hara et al., 2006). Several particles do not have a satellite structure in Fig. 4a. In contrast to the dominance of satellite particles in the summer, aerosol particles with solid materials and without a satellite structure were dominant during winter–spring, as shown in Fig. 4b. Although aerosol particles without a satellite structure were usually dominant during winter–spring in this study,

ACPD
13, 8153–8211, 2013

the number density of aerosol particles with a satellite structure increased occasionally in the lower boundary layer during winter–spring, as shown in Fig. 4c.

Figure 5 depicts examples of EDX spectra of aerosol particles collected over Syowa Station. In this study, carbon-coated collodion thin film on the Ni-grid was used as the sample substrate, so that strong background peaks of C, O, and Ni were obtained in EDX analysis. These elements were excluded from discussion. In addition, the strong carbon peak hampers identification and determination of N in EDX analysis. In Fig. 5a, Na, Mg, S, Cl, K, and Ca were detected from aerosol particle. Because the atomic ratio of these elements was close to the atomic ratio in seawater, this particle might be identified as sea-salt particles with less sea-salt modification. Although aerosol particle in Fig. 5b had similar constituents to particle in Fig. 5a, the relative peak height of Mg to Na was higher than that in seawater and sea-salt particle in Fig. 5a. This particle might be identified as Mg-enriched sea-salt particles. Mg-enrichment in sea-salt particles was observed in winter–spring at Syowa Station, Antarctica (Hara et al., 2005, 2010a). Details of sea-salt fractionation are discussed later (Sect. 3.7). Major elements of aerosol particle in Fig. 5c were Na and S. Cl^- in sea-salt particles can be depleted through heterogeneous reactions with acidic species during the summer, as explained by Mouri et al. (1999) and Hara et al. (2005). Therefore, the particle in Fig. 5c is identifiable as wholly Cl^- depleted sea-salt particles modified by acidic sulfur species such as SO_4^{2-} and $CH_3SO_3^-$. Hereinafter, we designate particles of this type as "modified sea-salt particles". Aerosol particle in Fig. 5d contained Na, Cl, and K. Unlike sea-salt and modified sea-salt particles in Fig. 5a–c, the atomic ratios of Cl and K were higher than the seawater ratio. A K-Cl rich particle was obtained only once in an aerosol sample in coarse mode collected at 615 m on 10 May, 2005.

Aerosol particle in Fig. 5e consist of S. In addition, aerosol particles containing only S (as shown in Fig. 5e) had a satellite structure on the substrates. This particle might be a sulfate particle. According to previous works using chemical tests (Yamato et al., 1987) and laser microprobe techniques (Hara et al., 1995), sulfate particles in the Antarctic troposphere were composed predominantly of H_2SO_4 and were mixed in-

ACPD
13, 8153–8211, 2013

ternally with $CH_3SO_3^-$. Consequently, major components of the particle in Fig. 5e might be acidic sulfates related to ocean bioactivity. Because EDX can provide only elemental information, mixing states of SO_4^{2-} and $CH_3SO_3^-$ were not identified in this study. Hereinafter, we designate particles of this type as "sulfate particles". Aerosol particle in Fig. 5f contained S and K. These particles might be sulfates containing K. In contrast to "sulfate particles", sulfate particles containing K showed no satellite structure. Although sulfate particles in the Antarctic troposphere were derived predominantly from bioactivity in the ocean during the summer (e.g. Minikin et al., 1998), sulfate containing K cannot be released from oceanic bioactivity and cannot be formed by new particle formation and gas-to-particle conversion from aerosol precursors. Okada et al. (2001, 2008) reported that sulfates containing K are present even in the free troposphere in the Southern Hemisphere and that they were released from combustion sources such as biomass burning. Indeed, aerosol particles from biomass burning on South America and southern Africa can be transported to Antarctic coasts (Fiebig et al., 2009; Hara et al., 2010a). Consequently, aerosol particles depicted in Fig. 5f might be particles of combustion origin. In Fig. 5g, Mg and S were detected from EDX analysis. Atomic ratios of Mg and S were 52 and 48 %, respectively, in Fig. 5g; the particle might be composed predominantly of $MgSO_4$. Mg and Cl were detected from the aerosol particle in Fig. 5h. This particle was observed once in fine mode on 30 September. From the atomic ratio of Mg and Cl, the particle was inferred as $MgCl_2$. The aerosol particle in Fig. 5i contained Al, Si, S, K, Ca, Mn, and Fe. Because staining of aqueous solution was observed clearly around the solid particle in SEM image, this particle might be a mineral particle coated by sulfates. In Fig. 5j, Na, Mg, S, Cl, and Ca were detected in EDX analysis. This particle might be an internal mixture of sea-salt (or Mg-enriched sea-salt) and $CaSO_4$.

3.4 Vertical and seasonal features of aerosol constituents over Syowa Station

Aerosol particles of several types were identified in this study as shown in Fig. 5. The following sections present seasonal features and vertical features of aerosol con-

ACPD
13, 8153–8211, 2013

stituents (sea-salt particles, aerosol particles containing sulfates, and mineral particles). For quantitative discussion, the relative abundance was estimated from the results of EDX analyses, as shown in Fig. 6.

3.4.1 Sea-salt particles

In coarse mode, sea-salt particles were dominant in the lower troposphere throughout the year. Modified sea-salt particles in coarse mode were observed mainly during the summer. Additionally, Cl-depletion from sea-salt particles containing Cl proceeded partly during the summer (details are presented in Sect. 3.6). During winter–spring, sea-salt particles were strongly dominant in coarse mode in both the boundary layer and lower free troposphere. Because of frequent cyclone approaches during winter–spring, sea-salt particles might be lifted up to the free troposphere under storm conditions. Indeed, previous airplane-borne aerosol measurements by Yamanouchi et al. (1999) presented high aerosol enhancement in the free troposphere over Syowa Station immediately after storm conditions. As shown in our previous investigations (Hara et al., 2004, 2010a, 2011a), sea-salt particles were usually dominant near the surface under the strong wind conditions at Syowa Station during winter–spring.

Relative abundance of sea-salt particles and modified sea-salt particles in fine mode was < 2–12.5 % in the boundary layer during January–mid-March, although sea-salt particles and modified sea-salt particles were occasionally not obtained in samples taken in the free troposphere (e.g. 26 January, 16 February, 5 March, and 14 March). In January–mid-March, the modified sea-salt particles were dominant in fine mode, compared to coarse sea-salt particles. Relative abundance of sea-salt particles increased gradually in fine mode from mid-March, and the relative abundance of the modified sea-salt particles decreased. Sea-salt particles (containing Cl) were the most abundant aerosol constituents during the winter (abundance, ca. 90 %) in the boundary layer, although low abundance of sea-salt particles was occasionally observed in the winter (e.g. 19 May, 16 June, and 28 June), as shown in Fig. 4c. Earlier near-surface investigations at Syowa Station (Hara et al., 2004, 2010a, 2011) and Neumayer Station

ACPD
13, 8153–8211, 2013

(Weller et al., 2011) revealed a dominance of sea-salt particles and high abundance of non-volatile particles (probably sea-salt particles) during winter–spring. Sea-salt particles were dominant in the free troposphere during the winter on 28 May and 28 July. Because of occasional failure of aerosol sampling at the highest altitudes (free troposphere), however, vertical features of the sea-salt particles in the free troposphere during the winter were uncertain. The relation between vertical features of aerosol constituents and the air mass history is discussed in Sect. 3.5. Furthermore, the modified sea-salt particles were rarely observed in the winter in this study. The relative abundance of the modified sea-salt particles increased gradually again after September. This seasonal variation of sea-salt and modified sea-salt particles was similar to that described by Mouri et al. (1999) and by Hara et al. (2005). Details of sea-salt modification are discussed in Sect. 3.6.

3.4.2 Aerosol particles containing sulfates

High abundance of sulfate particles in coarse mode was observed in the boundary layer and lower free troposphere during summer–autumn. Particularly, sulfate particles in coarse mode were dominant in the lower free troposphere during the summer (26 January, 16 February, 5 March, 5 December, and 11 December). The relative abundance of sulfate particles in fine mode mostly exceeded 90 % in both the boundary layer and free troposphere during the summer. The sulfate particle dominance persisted until the end of March, when the relative abundance of sea-salt particles and modified sea-salt particles increased. Thereafter, the abundance of sulfate particles increased again in October, and reached >95 % at the end of November in both the boundary layer and free troposphere. Considering that the CN enhanced layer was observed often during the summer (Hara et al., 2011b), condensable vapors such as gaseous H_2SO_4 and CH_3SO_3H might be enhanced in the free troposphere. Indeed, DMS oxidation and accumulation in the free troposphere and buffer layer were reported by Legrand et al. (2001) and by Preunkert et al. (2008). The concentrations of aerosol precursors might increase to enable new particle formation in the free troposphere,

ACPD
13, 8153–8211, 2013

with subsequent particle growth through condensation of the condensable vapors, and coagulation during transport.

Although sea-salt particles and modified sea-salt particles were dominant during the winter, the relative abundance of sea-salt particles decreased occasionally in the boundary layer even in winter, as described above. Higher abundance of sulfate particles (approximately 80 %; some examples are 19 May, and 16 and 28 June, 2005) in the boundary layer during the winter corresponded to the lower relative abundance of sea-salt particles. Particularly high abundance of sulfate particles in the winter was obtained in the surface inversion layer and lower boundary layer. Details of higher relative abundance of sulfate particles during winter–spring are discussed later in Sect. 3.5.2.

K-rich sulfate particles were distributed mostly in fine mode, except in March–May, July, and October, and were identified in the boundary layer and free troposphere in this study. Relative abundance of K-rich sulfate particles in fine mode ranged from "not-detected" to 2.4 % (< 1 % in most cases). According to Okada et al. (2008), K-rich sulfate particles, which can be released from combustion of biomass and bio-fuel, were distributed in the free troposphere of Southern Hemisphere in the austral winter (July). Furthermore, Hara et al. (2010a) and Fiebig et al. (2009) reported that aerosol particles from biomass burning in South America and southern Africa were transported to the Antarctic coast. With the exception of January–February, seasons with identification of K-rich sulfate particles corresponded well to seasons with high abundance of plume outflow from South America and southern Africa (Hara et al., 2010a). Consequently, K-rich sulfate particles over Syowa Station might be supplied by long-range transport from combustion processes in middle and lower latitudes such as South America and southern Africa. In spite of low abundance of plume outflow, K-rich sulfate particles were identified even in January and February in this study. Backward trajectory (see Supplement) showed that air masses containing K-rich sulfate particles in January and December came from the free troposphere over the Antarctic continent without significant combustion sources. Previous model studies (Koch and Hansen, 2005; Stohl and Sodemann, 2010) presented transport from low latitudes and middle latitudes to

ACPD
13, 8153–8211, 2013

the Antarctic regions through the upper free troposphere. Considering the high BC concentration at the South Pole in the summer (Bodhaine, 1995), we must discuss the likelihood of transport of combustion-origin aerosols through the upper troposphere during the summer. For better understanding of transport processes of combustion-origin particles such as K-rich sulfate particles, we must obtain more knowledge related to aerosol constituents in the upper free troposphere and the Antarctic continent.

Mg-rich sulfate ($MgSO_4$) particles were distributed only in fine mode in this study. Relative abundance of Mg-rich sulfate particles ranged from "not detected" to 1.9 %. Mg-rich sulfate particles were identified in samples obtained during January–mid-May, 4 September and October–December so that variations of Mg-rich sulfates might have strong seasonality along the Antarctic coasts. In addition, Mg-rich sulfate particles were observed dominantly in samples taken in the boundary layer. Analysis of backward trajectories (see Supplement) showed that air masses containing Mg-rich sulfate particles were transported over the Antarctic continent and coastal areas in the most cases. A similar transport pathway, however, was observed in air masses without Mg-rich sulfates during the winter, which implies that the presence of Mg-rich sulfate particles might be associated not only with the transport pathway but also with seasonal features of the origin of Mg-rich sulfates. To our knowledge, Mg-rich sulfate particles have never been identified in aerosol particles in the Antarctic troposphere, although $MgSO_4$ microparticles and Mg-rich particles were obtained in ice cores and surface snow taken in the Antarctic plateau (Ohno et al., 2005; Iizuka et al., 2006, 2012). As described above, $MgCl_2$ particles were observed only on 30 September in this study. In addition, $MgCl_2$ was identified at Comandante Ferraz Station at King George Island (Artaxo et al., 1992). Considering that $MgCl_2$ can be converted to $MgSO_4$ through heterogeneous reactions with gaseous sulfur species as well as sea-salt modification, $MgCl_2$ and Mg-rich sulfate particles might be released from the same origin. Although results of our previous studies showed that Mg was enriched in fractionated sea-salt particles originating from sea-ice during winter–spring (Hara et al., 2010a, 2012), $MgSO_4$ particles were not identified during winter–spring. Therefore, $MgSO_4$ particles and Mg-rich

ACPD
13, 8153–8211, 2013

particles might not originate from sea-salt fractionation on sea-ice during winter–spring but from other sources during the summer. Details of sea-salt fractionation and origins of Mg-rich particles are discussed in Sect. 3.7.

3.4.3 Mineral particles

Mineral particles in coarse and fine modes were identified in the boundary layer and lower free troposphere throughout the year. Relative abundance of aerosol particles containing minerals was from not-detected to approximately 50 % in coarse mode, and from not-detected to approximately 4 % in fine mode. A dry soil surface appeared partly in Ongul Islands during the end of December–early February. Therefore, mineral particles in the boundary layer might be affected by local emissions in addition to long-range transport. Local emission of mineral particles, however, can be negligible during the end of February–early December because the soil surface was covered with snow. According to Wagenbach (1996) and Weller et al. (2008), seasonal variations of mineral particles showed maximum values in the summer at Neumayer Station. Previous investigations revealed that the cyclonic system engenders long-range transport of mineral particles to the Antarctic coasts (Pereira et al., 2004; Hara et al., 2010a; Li et al., 2010). Considering the presence of mineral particles in the boundary layer and the free troposphere found in this study and in a previous investigation (Pereira et al., 2004; Hara et al., 2006, 2010a; Weller et al., 2008; Li et al., 2010), mineral particles might be supplied by long-range transport to Syowa Station through the boundary layer and free troposphere.

3.5 Relation between transport processes and vertical features of aerosol constituents

As described above, vertical features of aerosol constituents in the winter–spring are likely to be associated with the air mass history. In this section, we specifically examine

ACPD
13, 8153–8211, 2013

the relation between air mass history and dominance of sea-salt particles and sulfate particles in the lower troposphere during winter–spring.

3.5.1 Dominance of sea-salt particles in the lower troposphere

High relative abundance of sea-salt particles was observed in the lower troposphere during winter–spring, particularly on 28 May. As shown in Fig. 3c, air parcels at sampling altitudes on 28 May came from the boundary layer (< 500 m) at 51–60° S, which is over the ocean in a sea-ice area. This poleward pathway was associated with approach of a cyclone, which passed to the north of Syowa Station before the tethered balloon observation on 28 May 2005. With poleward flow and vertical mixing, sea-salt particles might be distributed in the lower free troposphere in the case of 28 May. Furthermore, remarkable aerosol enhancement (Antarctic haze) was observed near the surface at Syowa Station during 24–27 May 2005 (Hara et al., 2010a). Although the aerosol number concentrations of $D_p > 0.3\,\mu m$ were approximately $5000\,L^{-1}$ in the boundary layer on 28 May, the number concentrations reached $20\,258\,L^{-1}$ at 1300 m (Hara et al., 2011b). Consequently, the aerosol enhanced condition (Antarctic haze) persisted in the lower free troposphere on 28 May. Aerosol enhancement by vertical mixing was obtained over Syowa Station immediately after the cyclone's passing (Yamanouchi et al., 1999). Similar to the Antarctic haze condition near the surface (Hara et al., 2010a), sea-salt particles were major constituents in the aerosol enhanced layer in the case of 28 May, as depicted in Fig. 6.

Fortunately, more tethered balloon measurements were taken under the aerosol-enhanced condition immediately after the Antarctic haze on 22 July (Hara et al., 2010a, 2011b). In contrast to data obtained on 28 May, high aerosol number concentrations (approximately $12\,463\,L^{-1}$ in $D_p > 0.3\,\mu m$) were obtained only in the boundary layer (surface–ca. 600 m) on 22 July (Hara et al., 2011b). In addition, sea-salt particles were predominant in the boundary layer, whereas high abundance of sulfate particles was observed in the free troposphere. Air masses had come mostly from the boundary layer

ACPD
13, 8153–8211, 2013

sea-ice regions 2–3 days prior (see Supplement). Higher relative abundance of sea-salt particles on other days (e.g. 4 September) was found also in air masses transported from the boundary layer over the Southern Ocean and sea-ice regions. Moreover, sea-salt particle dominance was coincident with higher aerosol number density over Syowa Station (Hara et al., 2011b). Similar to the case on 28 May, strong winds were observed at Syowa Station by the cyclone approach before aerosol enhanced conditions and sea-salt particle dominance. Therefore, strong wind conditions attributable to the cyclone approach might engender a significant release of sea-salt particles from surface of sea-ice and ocean by wind-blowing processes. Because strong winds were observed usually at Syowa Station during winter–spring (Sato and Hirasawa, 2007), high abundance of sea-salt particles might be typical in the boundary layer, as described by Hara et al. (2004, 2010a, 2011a).

3.5.2 Dominance of sulfate particles in the lower troposphere during winter–spring

Although sea-salt particles were dominant near the surface during winter–spring as described above, high relative abundance of sulfate particles was observed occasionally in the near surface to the lower boundary layer (< 500 m), even during winter (e.g. 10 May, 19 May, 16 June, 28 June, 18 August), as depicted in Fig. 6. In contrast to the dominance of sea-salt particles in high aerosol number density, high relative abundance of sulfate particles was coincident with the lower aerosol number density (Hara et al., 2011b). For instance, the relative abundance of sulfate particles was approximately 80 % in fine mode below 500 m on 16 June 2005, whereas relative abundance of sea-salt and modified sea-salt particles increased by 60 % above 700 m (Figs. 4 and 6). In addition, higher potential temperature and relative humidity were observed at altitudes greater than 700 m (Fig. 2). Backward trajectory from the sampling altitudes on 16 June revealed that air masses below 500 m were transported from the free troposphere over Antarctic continent, whereas air masses above 700 m came from the boundary layer over the ocean (55–60° S). Consequently, this profile and air mass history strongly

ACPD
13, 8153–8211, 2013

suggest that warm and humid oceanic air masses mixed with a large amount of sea-salt particles flowed into the upper boundary layer–lower free troposphere over Syowa Station. It is noteworthy that the tethered-balloon operation was conducted only under conditions of calm winds and high pressure. Remarkably high abundance of sulfate particles during the winter might appear over Syowa Station under high-pressure conditions. This result was closely coincident with the high abundance of volatile particles near the surface in air parcels from the free troposphere over the continent during the winter (Hara et al., 2011a). Consequently, sulfate particles might be dominant in the free troposphere over the Antarctic continent and coasts during winter–spring. In the other cases with high abundance of sulfate particles in the lower troposphere during winter–spring, air masses had fallen from the free troposphere over the continent or coasts. This suggests that aerosol particles in the free troposphere had flowed to the boundary layer in the Antarctic coasts under high-pressure conditions during winter–spring.

3.6 Seasonal and vertical variations of sea-salt modification

As depicted in Fig. 6, modified sea-salt particles were identified in both the boundary layer and free troposphere, particularly during the summer. Although seasonal features of sea-salt modification near surface at Antarctic coasts were shown by Mouri et al. (1999) and Hara et al. (2004, 2005), vertical gradients of sea-salt modification have never been reported for Antarctic regions. Seasonal and vertical features of sea-salt modification are examined in this section.

3.6.1 Seasonal variations of sea-salt modification in coarse mode

Figure 7 depicts examples of ternary plots of sea-salt constituents (Na, S and Cl) in coarse mode. Sea-salt particles internally mixed with mineral particles were excluded from Fig. 7 to avoid misunderstanding of the sea-salt chemistry. In this study, internal mixtures of sea-salts and minerals were few or none in each sample. Green and

ACPD
13, 8153–8211, 2013

blue stars respectively denote atomic ratios of bulk seawater ratios and wholly Cl depleted sea-salt particles by sulfates. The red line represents the stoichiometric line from the sea salt particles with bulk seawater ratio to the Cl-depleted sea salt particles by sulfates. When Cl in sea-salt particle is replaced stoichiometrically to SO_4^{2-} by heterogeneous reactions, each sea salt particle is distributed along the stoichiometric line.

Many sea-salt particles at 306 m on 16 February (Fig. 7a) and 408 m on 28 November (Fig. 7h) were distributed along the stoichiometric line, so that sea-salt particles might be modified dominantly with sulfates. By contrast, sea-salt modification in coarse mode was insignificant in the boundary layer and free troposphere during the winter, as described similarly by Mouri et al. (1999) and Hara et al. (2005). The sea-salt particles at 47 m on 23 April (Fig. 7b) were distributed remarkably close to the seawater ratio. Although significant sea-salt modification was not identified in the upper boundary layer (353–806 m) on 23 April (see Supplement), the modified sea-salt particles and sea-salt particles with lower Cl atomic ratio were observed at 934 m (Fig. 7c), which was near a cloud base. Because sea-salt particles near the cloud base were distributed along the stoichiometric line, sea-salt particles might be modified with sulfates. Sea-salt modification near the cloud base might be promoted also through (1) preferential heterogeneous reactions under high relative humidity and (2) coagulation of acidic sulfate particles.

Although the atomic ratio of sea-salt particles at 47 m on 23 April (Fig. 7b) was close to the seawater ratio, the atomic ratio of Cl in sea-salt particles dropped to 40–45 % in most cases in coarse mode during winter–spring. We checked analytical conditions using artificial particles of pure NaCl and Na_2SO_4, but the analytical bias in EDX analysis cannot account for this difference. The slight decrease of Cl atomic ratio might result from sea-salt modification. The atomic ratio of S changed only slightly in the slightly modified sea-salt particles. Therefore, the likelihood of sea-salt modification with acidic gases other than sulfates should be considered. Previous investigations pointed out sea-salt modification by NO_3^- (Mamane and Gottlieb, 1992; Hara et al., 1999) and or-

ACPD
13, 8153–8211, 2013

ganic acids (Laskin et al., 2012). The NO_3^- concentration was higher than those of organic acids such as formate, acetate, and oxalate at Syowa Station during winter–spring (e.g. Hara et al., 2010a). Here, we attempt to estimate the NO_3^- concentration to engender a decrease of several to 10 % in Cl atomic ratio in coarse sea-salt particles, assuming that chemical constituents were homogeneous in sea-salt particles and that NO_3^- causes sea-salt modification. Using the Cl atomic ratio and bulk Na^+ concentrations in the coarse mode obtained from bulk analysis (e.g. Hara et al., 2004, 2010a), the range of NO_3^- concentration was estimated as ca. 0.2 nmol m^{-3}. The estimated NO_3^- concentration was consistent with ambient NO_3^- concentration in coarse mode ranging in below the detection limit (BDL) – 0.4 nmol m^{-3} (annual mean, 0.04 nmol m^{-3}) at Syowa Station (Hara et al., unpublished data). Therefore, slight sea-salt modification in coarse mode might occur to a marked degree through heterogeneous NO_3^- formation during winter–spring. The small contribution of NO_3^- to sea-salt modification implies lower concentrations of NO_3 precursors such as HNO_3, N_2O_5, and NO_3 and high sea-salt concentration in the lower troposphere around the Antarctic coasts.

3.6.2 Seasonal variations of sea-salt modification in fine mode

Figure 8 presents examples of ternary plots of sea-salt constituents (Na, S and Cl) in fine mode. As with the plots in coarse mode, sea-salt particles containing minerals were removed from Fig. 8. Compared to coarse sea-salt particles, sea-salt constituents were distributed widely in fine mode over Syowa Station. This suggests that sea-salt modification occurs preferentially in fine mode. A similar tendency was observed in previous investigations in Antarctic and Arctic regions (Mouri et al., 1999; Hara et al., 2002, 2005; Rankin and Wolff, 2003). On 12 February (Fig. 8a) and 11 December (Fig. 8i), many sea-salt particles containing Cl were distributed around the stoichiometric line. Moreover, some sea-salt particles containing Cl had a significantly larger S ratio relative to the stoichiometric line for example on 23 April (Fig. 8c) and 11 December (Fig. 8i), so that these sea-salt particles might be modified not only with SO_4^{2-} but also

ACPD
13, 8153–8211, 2013

with $CH_3SO_3^-$ as suggested by Hara et al. (2005). The most of the modified sea-salt particles were distributed in Cl ratio of ca. 0 % and higher S atomic ratio relative to the modified sea-salt particles (marked by blue stars), especially 16 February (Fig. 8b). These distributions strongly suggest (1) sea-salt modification, predominantly with sulfates and methanesulfonate, and (2) occurrence of excess sulfate/methanesulfonate formation on the modified sea-salt particles through the heterogeneous reactions and coagulation during the summer. The presence of the modified sea-salt particles containing excess sulfates implies that sea-salt particles can act as important scavengers of condensable vapors and aerosol precursors such as H_2SO_4 gas.

Although sea-salt modification was not significant in coarse mode in March–October (as shown in Fig. 7), partly Cl-depleted sea-salt particles and the modified sea-salt particles were often identified in fine mode during winter–spring. Insignificant sea-salt modification corresponded to high abundance of sea-salt particles under aerosol enhanced conditions (Antarctic haze, e.g. 28 May, 22 July, and 30 September). Because of higher S atomic ratio in partly Cl-depleted sea-salt particles and the modified sea-salt particles, acidic sulfur species (predominantly SO_4^{2-}) might cause sea-salt modification in fine mode during winter–spring. Similar to coarse sea-salt particles, the Cl atomic ratio decreased slightly without increase of S atomic ratio in fine mode relative to the seawater ratio, so that sea-salt particles might be modified with NO_3^- also in fine mode during winter–spring.

Significant Cl depletion from sea-salt particles occurred on 18 August, as shown in Fig. 8e, f. Sea-salt particles and the modified sea-salt particles, however, were distributed in lower S ratio relative to the stoichiometric line. Particularly, the modified sea-salt particles and partly Cl-depleted sea-salt particles were distributed mostly in < 20 % of S in atomic ratio at 674 m on 18 August (Fig. 8e). As discussed earlier, sea-salt particles on 18 August might be modified significantly by heterogeneous NO_3^- formation in addition to sea-salt modification partly by sulfur species such as SO_4^{2-}. Furthermore, previous investigations (Mouri et al., 1999; Hara et al., 2005) revealed the high contribution of NO_3^- to sea-salt modification at Syowa Station in August. Such a high con-

ACPD
13, 8153–8211, 2013

tribution of NO_3^- to sea-salt modification was observed only during August–September in this study. Furthermore, more sea-salt particles were modified dominantly by NO_3^- in the free troposphere on 18 August (Fig. 8f). Backward trajectory on 18 August (see Supplement) showed that air masses of each sampling altitude had travelled over the Antarctic coast along the coastline without marked vertical mixing during the prior 5 days. Therefore, the modified sea-salt particles at 1430 m might have travelled for at least 5 days in the free troposphere. Consequently, the marked sea-salt modification by NO_3^- implies that the concentrations of NO_3^- precursors such as HNO_3, N_2O_5, and NO_3^- are enhanced in the boundary layer and lower free troposphere over the Antarctic coast during August–September.

3.6.3 Vertical features of sea-salt modification in coarse mode

Figures 9 and 10 portray vertical features of atomic ratios of Cl/Na and S/Na in coarse sea-salt particles over Syowa Station. Because of the lower number concentrations in coarse mode during January–February and mid-November–December (Hara et al., 2011b), the vertical features of sea-salt modification in coarse mode were uncertain except for the cases on 16 February and 28 November. For 16 February, median Cl/Na and S/Na ratios were ca. 0.75 and 0.05–0.08, respectively, above 500 m (the upper boundary layer), whereas the median Cl/Na ratio dropped to ca. 0.5 at 306 m and the median S/Na ratio increased by 0.25. As Fig. 7a shows, sea-salt particles might be modified dominantly with SO_4^{2-} at 306 m on 16 February. Relative humidity on 16 February (Fig. 2) reached higher than 70 % in the boundary layer and lower than 50 % above the boundary layer. Although air masses at each sampling height on 16 February were transported from the free troposphere over the Antarctic continent and coastal regions before 5 days (see backward trajectory in Supplement), no significant difference of air mass origins at each sampling altitude was identified in the backward trajectory.

Unlike to the vertical features of Cl/Na ratios on 16 February, Cl/Na ratios in sea-salt particles tended to increase in the upper boundary layer on 28 November. Particu-

ACPD
13, 8153–8211, 2013

larly, the median Cl/Na ratio dropped to 0.5 at 600 m. Although the median Cl/Na ratio was approximately 0.75 at the highest altitude (811 m), the ratio at the highest altitude includes great uncertainty because only several sea-salt particles were analyzed in the sample. Similar to the case on 16 February, a higher S/Na ratio was observed at altitudes with lower Cl/Na ratios. No significant difference of air mass origins in each sampling altitude was identified in the 5-day backward trajectory analysis of 28 November. According to Hara et al. (2002), sea-salt modification preferred to proceed under conditions with higher relative humidity and higher concentrations of acidic gases in the well-mixed boundary layer. As shown in Fig. 2, lower Cl/Na ratios in coarse mode corresponded to higher relative humidity (e.g. 306 m on 16 February; 408, 615, and 811 m on 28 November). Consequently, the relative humidity around aerosol particles might affect heterogeneous reactivity on sea-salt particles in the Antarctic troposphere, although vertical distributions of the concentrations of gaseous acidic species must be considered.

In contrast to the appearance of lower Cl/Na ratio during the summer, median Cl/Na ratios in coarse mode were 0.75–1.3 in the boundary layer and the free troposphere during winter–spring, except in the sample collected near or in a cloud layer (934 m) on 23 April. Median S/Na ratios in coarse mode ranged mostly in ca. 0.05 during winter–spring except the samples collected at 47 m and 934 m on 23 April. Furthermore, variation of Cl/Na and S/Na ratios became smaller during winter–spring. Higher Cl/Na ratios than 1 were observed occasionally in the boundary layer (e.g. 23 April, 19 May, 22 July and 4 September). Particularly, median Cl/Na ratios at 47 m on 23 April reached ca. 1.35 (mean ratio, ca. 1.30). Because Cl/Na ratios in seawater (e.g. Wilson, 1975) are ca. 1.18, the higher Cl/Na ratio suggests strongly that Cl was enriched in sea-salt particles by sea-salt fractionation during winter–spring, as reported by Hara et al. (2012). By contrast, the Cl/Na ratio (ca. 0.75) in most cases was slightly lower than the seawater ratio. As discussed in Sect. 3.6.1, this might result from slight sea-salt modification with NO_3^-.

ACPD
13, 8153–8211, 2013

3.6.4 Vertical features of sea-salt modification in fine mode

Figures 11 and 12 portray vertical features of atomic ratios of Cl/Na and S/Na in fine sea-salt particles over Syowa Station. Median Cl/Na and S/Na ratios in sea-salt particles and the modified sea-salt particles ranged mostly in < 0.2 and > 0.5, respectively, in the boundary layer and lower free troposphere during the summer. This implies that fine sea-salt particles preferred to be modified relative to coarse sea-salt particles in both boundary layer and lower free troposphere especially in January–mid-March and mid-November–December. Because lower Cl/Na ratios were found in higher S/Na ratios in the boundary layer and the free troposphere, acidic sulfur species such as SO_4^{2-} and $CH_3SO_3^-$ might contribute to sea-salt modification in fine modes, as discussed in Sect. 3.6.2. Although higher Cl/Na ratios were obtained at altitudes greater than 500 m on 5 December, 2005, air masses with higher Cl/Na ratios were transported from the boundary layer over the ocean during the prior 5 days. Conversely, lower Cl/Na ratios in the most cases during the summer corresponded to transport from the Antarctic coasts–continents during the prior 5 days. Consequently, the vertical features might be attributed to the air mass history and aging time of sea-salt modification. From comparison between Cl/Na ratios and air mass history, it appears to take longer than 5 days for complete Cl depletion in fine sea-salt particles around the Antarctic coasts during the summer.

Although the median Cl/Na ratio in coarse mode was greater than 0.75 during April–November, a lower median Cl/Na ratio and large variance of Cl/Na ratio were identified in the boundary layer and lower free troposphere even in the winter. This suggests strongly that sea-salt modification proceeded with preference in fine mode in the boundary layer and lower free troposphere even during winter–spring over Syowa Station. As shown in Fig. 11, vertical features of median Cl/Na ratios in fine sea-salt particles during winter–spring are classifiable as (1) almost constant Cl/Na ratios (e.g. 28 May, 22 July, 30 September), (2) lower Cl/Na ratios in the lower boundary layer (e.g.

ACPD
13, 8153–8211, 2013

19 May, 16 June, 28 June, and 17 September), or (3) lower Cl/Na ratios in the upper boundary layer and lower free troposphere (e.g. 10 May, 18 August, and 4 September).

In the first type, vertical features of variation of Cl/Na ratios in fine mode tended to be smaller. The median Cl/Na and S/Na ratios were approximately 0.75–0.80 and < 0.2, respectively, in the boundary layer and lower free troposphere. This type was observed in the cases of higher relative abundance of sea-salt particles in the boundary layer under aerosol enhanced conditions (Antarctic haze), as depicted in Fig. 6. The backward trajectory shows that air masses came from ocean and sea-ice regions to the observed area over Syowa Station during the prior 5 days. Therefore, sea-salt emissions from the ocean surface and sea-ice and rapid transport to Syowa Station might cause some slight sea-salt modification in the boundary layer and lower free troposphere. With the suggestion of dominance of sea-salt particles (Hara et al., 2004) and slight sea-salt modification during the winter (Hara et al., 2005, 2010a), the first type might be dominant under usual winter conditions with stronger winds.

In the second type, lower Cl/Na ratios were observed remarkably in the lower boundary layer on 19 May, 16 June, 28 June, and 17 September, when higher abundance of sulfate particles was obtained in the boundary layer. In spite of the appearance of sea-salt particles with lower Cl/Na ratios in the lower boundary layer, the median Cl/Na ratios reached 0.7–0.9 in the upper boundary layer and lower free troposphere. As shown in the backward trajectory on 16 June (Fig. 3), sea-salt particles with lower Cl/Na and high S/Na ratios below 500 m were present in air masses from the free troposphere over the Antarctic continent, whereas air masses with higher Cl/Na ratio came from sea-ice and ocean areas. A similar air mass history was obtained in the other cases of the second type. Additionally, median S/Na ratios in fine mode increased by 0.3–0.6 in the lower boundary layer, as depicted in Fig. 12. Moreover, ternary plots of sea-salts (Na, S and Cl) in the second type imply that SO_4^{2-} makes a substantial contribution to sea-salt modification in fine mode (Fig. 8g and Supplement). Considering that the high Cl/Na and lower S/Na ratios in the sea-salt particles were obtained in the air masses transported ocean and sea-ice regions, the concentrations of gaseous

ACPD
13, 8153–8211, 2013

acidic sulfur species might be not sufficiently high to engender rapid sea-salt modification within several days. Acidic sulfur species such as SO_4^{2-} and $CH_3SO_3^-$ in aerosol particles are linked to oceanic biogenic activity in the coastal Antarctic regions during summer, but less so during the winter (e.g. Minikin et al., 1998; Moore and Abbott, 2002). Indeed, previous aerosol measurements showed a winter minimum of $CH_3SO_3^-$ concentration of aerosol particles at the Antarctic coasts (Osada et al., 1998; Minikin et al., 1998; Jourdain and Legrand, 2001) and inland stations (Weller et al., 2007; Preunkert et al., 2008). Nevertheless, significant sea-salt modification with acidic sulfur species (e.g. SO_4^{2-}) was obtained for air masses transported from the free troposphere over the continent in these cases. Measurements of sulfur aerosol precursors at Dumont d'Urville Station, Antarctica showed the presence of a large amount of DMS and DMSO in the winter (Jourdain and Legrand, 2001). In addition, higher concentrations of DMS were observed at Concordia Station on the high Antarctic plateau during the winter because of the longer life time resulting from lower solar radiation (Preunkert et al., 2008). Therefore, the dominance of acidic sulfate particles and a large amount of sulfur aerosol precursors might engender sea-salt modification by heterogeneous reactions and coagulation for longer suspension periods of sea-salt particles in the free troposphere over Antarctica. Under anticyclone conditions at Syowa Station, outflow of air masses in the free troposphere over the Antarctic continent to the boundary layer in the Antarctic coast might create vertical features of sea-salt modification in the second type.

In the third type, the vertical gradients of Cl/Na ratios were observed on 10 May, 18 August, and 4 September. Comparison with vertical features of meteorological data (Fig. 2) and aerosol number density (Hara et al., 2011a) shows the vertical gradients of Cl/Na ratios on 10 May and 4 September in the surface inversion layer and the boundary layer, although the gradient was observed in the boundary layer and lower free troposphere on 18 August. Median Cl/Na ratios in the surface inversion layer (< 350 m) on 10 May were approximately 0.4. They decreased gradually to 0 (mean, 0.2) in the upper boundary layer. On 4 September, median Cl/Na ratios changed gradually from

ACPD
13, 8153–8211, 2013

0.88 at 230 m to 0.57 at 850 m. With the vertical gradient of Cl/Na ratios, S/Na ratios increased gradually in the upper boundary layer on both days. Ternary plots (Na-S-Cl) on 4 September revealed a significant contribution of SO_4^{2-} to sea-salt modification in fine mode (see Supplement). Moreover, higher relative humidity was identified at altitudes with lower Cl/Na ratios. The relative humidity changed from ca. 45 % near the surface to ca. 94 % at 850 m on 4 September. Although sea-salt particles with lower Cl/Na ratios were distributed in the lower free troposphere, relative humidity reached 60–65 % at altitudes with lower Cl/Na ratios. Backward trajectories at each sampling altitude on 18 August showed transport in the lower free troposphere over the Antarctic coasts, so that the air mass history cannot account for the vertical gradient of Cl/Na. As suggested by previous investigations conducted by von Glasow and Sander, (2001) and by Hara et al. (2002), sea-salt modification occurs to a considerable degree under conditions with higher relative humidity. Therefore, the vertical gradients of Cl/Na and S/Na on 10 May and 4 September might result from enhancement of sea-salt modification under conditions with vertical gradients of relative humidity.

In addition to the third type, vertical gradients of relative humidity were observed also on 23 April and 16 June: 36–95 % on 23 April and 57–96 % on 16 June. Although median Cl/Na ratios were 0.6–0.75 in the upper boundary layer in both cases, some sea-salt particles with lower Cl/Na ratios (< 0.25) were present in the upper boundary layer. Backward trajectories (Fig. 3d; Supplement) showed that air masses with higher relative humidity approached from ocean and sea-ice areas within five days on 23 April and 16 June. A similar air mass history was identified on 28 May, as shown in Fig. 3c. Relative humidity, however, was 40–65 % in the boundary layer and free troposphere on 28 May. In contrast to cases on 23 April and 16 June, sea-salt particles with lower Cl/Na ratios (< 0.25) were not identified on 28 May. Consequently, the presence of sea-salt particles with lower Cl/Na ratios on 23 April and 16 June suggests that sea-salt modification was enhanced by higher relative humidity and that it might take longer than 5 days for sea-salt modification in the upper and lower free troposphere, even under higher relative humidity than that during winter–spring.

ACPD
13, 8153–8211, 2013

3.7 Seasonal variations of sea-salt fractionation

As shown in Fig. 5b, Mg-enriched sea-salt particles were occasionally identified in this study. As suggested by our previous studies (Hara et al., 2005, 2010a, 2012), Mg-enriched sea-salt particles might be associated with sea-salt fractionation. Seasonal variations of the fractionated sea-salt particles are discussed in this section.

3.7.1 Sea-salt fractionation in coarse mode

Figure 13 depicts examples of ternary plots of sea-salts (Na, Mg, and S) in coarse mode. Internal mixtures of sea-salts and minerals were removed from the ternary plots to avoid misunderstanding. In the ternary plots, sea-salt particles with bulk seawater ratio are distributed around the blue circle (bulk seawater ratio). When the sea-salt particles are modified by sulfate and not fractionated, they are distributed around the stoichiometric line between the blue circle (seawater ratio) and red circle (modified sea-salt ratio with sulfate). With sea-salt fractionation by precipitation of Na-salts such as mirabilite (Na_2SO_4 $10H_2O$) and hydrohalite (NaCl $2H_2O$) (Hara et al., 2012), Mg in sea-salt particles can be enriched gradually during winter–spring. In the case in which sea-salt fractionation (replacement between Na and Mg) occurs without sea-salt modification by sulfate, sea-salt particles are distributed around the stoichiometric line between the blue circle (bulk seawater ratio) and cyan circle ($MgCl_2$). When sea-salt fractionation and sea-salt modification by sulfate occur stoichiometrically and simultaneously, sea-salt particles are distributed around the stoichiometric line between the blue circle (seawater ratio) and green circle ($MgSO_4$).

Because sea-salt modification occurred during the summer, sea-salt particles were distributed around the stoichiometric line of sea-salt modification without sea-salt fractionation, as shown in Fig. 13a–g. The Mg ratios in coarse sea-salt particles ranged mostly from several percent to 20 % in the summer. On 23 March and 23 April, most sea-salt particles were distributed around the seawater ratio, although a slightly higher Mg ratio (ca. 20 %) was obtained in some sea-salt particles (Fig. 13b, c). The presence

ACPD
13, 8153–8211, 2013

of sea-salt particles with slightly high Mg enrichment suggests that sea-salt fractionation started to occur around Syowa Station in the end of March and April, when air temperatures near the surface dropped occasionally to lower than −9 °C (Hara et al., 2012). Sea-salt particles on 22 July were distributed markedly around the stoichiometric line of sea-salt fractionation without sea-salt modification. Although the median and mean Mg ratios of mineral-free sea-salt particles in this sample were 19.8 and 23.2, respectively, the highest Mg ratios were approximately 60 %, strongly suggesting that Mg was enriched in sea-salt particles by sea-salt fractionation. Similarly to 22 July, Mg enrichment was also observed on 30 September. High Mg enrichment in the winter–spring was identified also in bulk aerosol data at Syowa Station (Hara et al., 2012). Ternary plots of Na-Mg-S and Na-Mg-Cl (not shown) imply that Mg is present in coarse sea-salt particles as $MgCl_2$. Therefore, aerosol particles containing mostly $MgCl_2$ (Fig. 5h) might be associated with sea-salt fractionation on sea-ice.

3.7.2 Sea-salt fractionation in fine mode

Figure 14 shows examples of ternary plots of sea-salts (Na, Mg, and S) in fine mode. Mg ratios in fine sea-salt particles differed greatly from those in coarse mode. On 16 February (Fig. 14a), many sea-salt particles were distributed at Mg ratio ≈ 0 and the higher S ratios relative to the stoichiometric line between the blue circle and green circle. Similarly, sea-salt particles containing Mg were distributed around the stoichiometric line of sea-salt fractionation with sea-salt modification on 23 March and 23 April (Fig. 14b, c). With comparison with Mg ratio on 16 February, Mg ratio increased gradually on 23 March and 23 April. Particularly, the highest Mg ratio was ca. 40 % on 23 March and 78 % on 23 April in the ternary plots. In addition, the number of sea-salt particles with Mg ratio ≈ 0 tended to decrease. Hereinafter, we designate sea-salt particles with Mg ratio ≈ 0 as "Mg-free sea-salt particles". On 22 July (Fig. 14d), fine sea-salt particles were distributed dominantly around the stoichiometric line of sea-salt fractionation without sea-salt modification, as were coarse sea-salt particles (Fig. 13d). On 4 September (Fig. 14e), sea-salt particles were distributed around the stoichiometric line

ACPD
13, 8153–8211, 2013

of sea-salt fractionation without sea-salt modification and along with the stoichiometric line of sea-salt fractionation with sea-salt modification. Mg ratios in sea-salt particles were approximately 60 % on 22 July and 4 September. Large variation of Mg ratios suggests that sea-salt constituents were heterogeneous along the Antarctic coasts during winter–spring. Although Mg-free sea-salt particles were identified rarely in fine mode during May through August, the number of Mg-free sea-salt particles increased again in September (Fig. 14 and Supplement). On 28 November and 11 December (Fig. 14f, g), sea-salt particles were distributed around the stoichiometric line of sea-salt fractionation with sea-salt modification and Mg ratio ≈ 0. Therefore, sea-salt particles with Mg-free and Mg-enriched sea-salt particles were externally mixed in the Antarctic troposphere during the summer, as shown in the ternary plots (Fig. 14f, g). Furthermore, some particles were distributed around the ratio of $MgSO_4$ (green circle). The distribution around the stoichiometric line of sea-salt fractionation with sea-salt modification strongly suggests that $MgSO_4$ particles were derived from sea-salt fractionation and sea-salt modification.

Mg-enriched sea-salt particles can be formed through sea-salt fractionation by precipitation of mirabilite and hydrohalite on sea-ice under cold conditions (Hara et al., 2012), but Mg-free sea-salt particles cannot be formed. Indeed, Mg-free sea-salt particles were identified only rarely during the winter in this study. To explain the presence of external mixtures of $MgSO_4$ particles, Mg-rich sea-salt particles and Mg-free sea-salt particles in the summer, it is necessary to discuss Mg separation processes in the Antarctic regions that occur during the summer. Although sea-salt fractionation by Mg separation processes has not been identified, the likelihood of Mg separation in sea-salt particles was pointed out from continuous aerosol measurements near the surface at Syowa Station (Hara et al., 2012). Origins of Mg-free sea-salt particles, however, have not been discussed and understood in the Antarctic regions. Although sea-salt particles are released from open sea surface through bubble bursting, Mg-enrichment and Mg-depletion has never been identified in sea-salt particles produced by bubble bursting (Keene et al., 2007). Considering the seasonality of the presence of Mg-free

ACPD
13, 8153–8211, 2013

sea-salt particles, Mg separation in sea-salt particles might occur preferentially during the summer in the Antarctic regions. As described in Sect. 3.4.2, $MgSO_4$ particles were observed in air masses from the Antarctic continent and coasts. Indeed, $MgSO_4$ particles were identified in surface snow on the Antarctic continent (Iizuka et al., 2012) and ice core samples (Ohno et al., 2005; Iizuka et al., 2006). Therefore, we propose the hypothesis that Mg-separation proceeds in Antarctic regions during the summer. For better understanding of sea-salt fractionation by Mg separation, it is necessary to obtain a spatial distribution of sea-salt constituents from the Southern Ocean to the interior of the Antarctic continent during the summer.

3.7.3 Vertical features of fractionated sea-salt particles

Figures 15 and 16 respectively depict examples of vertical features of Mg/Na ratios in coarse and fine modes over Syowa Station. Although median Mg/Na ratios in coarse mode were mostly lower than 0.2 in the boundary layer and free troposphere during the summer (January–March and November–December), the median ratios in coarse mode were larger than 0.2 from April through October. During the winter, highly Mg enriched sea-salt particles in coarse mode (Mg/Na > 0.3) were occasionally identified in the boundary layer (e.g. 28 May and 22 July). In addition, the variation of Mg/Na ratios on 28 May was smaller in the air masses of the lower free troposphere, which were transported from the boundary layer above open sea areas. However, vertical features of Mg/Na ratios were not statistically significant in coarse sea-salt particles in most cases.

In contrast to Mg/Na ratio in coarse mode, median Mg/Na ratios in fine mode decreased occasionally to 0 during the summer because of the presence of Mg-free sea-salt particles. Sea-salt fractionation by Mg separation might engender greater variation of Mg/Na ratios in fine sea-salt particles during the summer. Median Mg/Na ratios in fine mode were greater than 0.2 from April through September. On 16 June, Mg/Na ratios were varied largely in the boundary layer (< 600 m) relative to the variations in the lower free troposphere (> 600 m), similar to the vertical features of Mg/Na ratios in

ACPD
13, 8153–8211, 2013

coarse mode. In addition, vertical features of Mg/Na ratios, however, were not statistically significant in fine sea-salt particles in most cases.

Variation of Mg/Na ratios tended to be larger in the summer than in winter in both coarse and fine modes. Seasonal features of the variation of Mg/Na ratios might be attributed to sea-salt fractionation such as Mg enrichment in the winter–spring and Mg separation in the summer. Compared to the vertical features of S/Na and Cl/Na ratios, vertical gradients of Mg/Na ratios were not significant in coarse or fine modes in the lower troposphere, perhaps because of (1) the slight change of Mg/Na ratios by sea-salt fractionation during the winter relative to Cl-loss, and (2) well dispersion and mixing of the fractionated sea-salt particles in the lower troposphere (< 2500 m) under observable conditions using the tethered balloon. To elucidate atmospheric cycles of sea-salt particles in the Antarctic regions, vertical features of the fractionated sea-salt particles must be examined under stronger wind conditions.

4 Summary and conclusions

Tethered balloon-borne aerosol measurements were conducted at Syowa Station, Antarctica during 2005. From single particle analysis using SEM-EDX, sulfate particles, sulfate particles containing K, $MgSO_4$ particles, $MgCl_2$ particles, sea-salt particles, Mg-enriched sea-salt particles, wholly Cl depleted sea-salt particles, Mg-free sea-salt particles, and mineral particles were identified in this study. Major aerosol constituents were sulfates during the summer and sea-salt particles during winter–spring in the boundary layer and free troposphere over Syowa Station. Sulfate particles containing K were identified mostly in fine mode except during March–May, July, and October in the boundary layer and free troposphere. As reported by Okada et al. (2008), Fiebig et al. (2009) and Hara et al. (2010), sulfate particles containing K might result from long-range transport after origination during combustion processes in South America and southern Africa. $MgSO_4$ particles were also mainly distributed in fine mode, and were obtained during January – mid-May, on 4 September, and during October–December.

ACPD
13, 8153–8211, 2013

Sulfate particles were major aerosol constituents in fine mode in both the boundary layer and free troposphere during the summer. In contrast to fine mode, sea-salt particles and the modified sea-salt particles were dominant in coarse mode in the boundary layer. High relative abundance of sulfate particles was obtained even in coarse mode in the lower free troposphere. Relative abundance of sea-salt particles increased in April in the boundary layer and lower free troposphere. Under the conditions with higher aerosol number density and air mass transport from the boundary layer over sea ice and Southern Ocean, the relative abundance of sea-salt particles reached $< 90\,\%$ in coarse and fine modes. Although high relative abundance of sea-salt particles was observed usually during winter–spring, higher relative abundance of sulfate particles was identified occasionally in the boundary layer even in the winter, for example, on 16 June and 28 June. Trajectory analysis suggests that sulfate particles in the boundary layer on 16 June and 28 June were transported from the free troposphere over the Antarctic continent and coast. When air mass in the free troposphere had descended into the boundary layer over Syowa Station, air masses with higher relative abundance of sea-salt particles were lifted from the boundary layer over sea-ice and the Southern Ocean to the upper boundary layer and lower free troposphere over Syowa Station.

Sea-salt particles in coarse and fine modes were modified mostly with SO_4^{2-} and $CH_3SO_3^-$ through the heterogeneous reactions during the summer. In addition, sulfates (and methanesulfonates) were enriched remarkably in the wholly Cl-depleted sea-salt particles, probably by condensation of H_2SO_4 and CH_3SO_3H gases and heterogeneous reactions with precursors. Furthermore, sea-salt particles were modified slightly with NO_3^-. It is noteworthy that NO_3^- made a significant contribution to sea-salt modification in the boundary layer and lower free troposphere in August. Vertical features of sea-salt modification during winter–spring were classified into (1) non-significant vertical features (less modification), (2) high modification in the lower boundary layer, and (3) high modification in the upper boundary layer and lower free troposphere. Insignificant vertical features of sea-salt modification were identified in cases of high aerosol number density, high relative abundance of sea-salt particles, and transport from sea-

ACPD
13, 8153–8211, 2013

ice and the Southern Ocean. This type might be typical conditions of vertical features of sea-salt modification during winter–spring. The second type was observed in cases of high relative abundance of sulfate particles in the lower boundary layer. Considering the air mass history in high relative abundance of sulfate particles during the winter, sea-salt particles might be modified gradually for longer than 5 days during their transport in the free troposphere. The third type was obtained in the well-mixed boundary layer with a strong vertical gradient of relative humidity. As suggested by previous works (von Glasow and Sander, 2001; Hara et al., 2003), sea-salt modification might be enhanced under conditions with higher relative humidity.

Mg-rich sea-salt particles were identified noticeably in coarse and fine modes during April–November through sea-salt fractionation on sea-ice. During the winter, Mg in sea-salt particles might occur in the form of $MgCl_2$. During late spring–summer, Mg-enriched sea-salt particles and Mg-free sea-salt particles were obtained in this study. The presence of Mg-free sea-salt particles cannot be explained by sea-salt fractionation on sea-ice during winter–spring. Consequently, Mg separation processes might occur in the Antarctic regions during late spring–summer, although specific processes remain unknown.

Supplementary material related to this article is available online at: http://www.atmos-chem-phys-discuss.net/13/8153/2013/acpd-13-8153-2013-supplement.pdf.

Acknowledgements. We would like to thank K. Matsubara (JARE46 leader, JMA), and K. Watanabe (JARE46 wintering leader; NIPR) for useful comments related to field operations around Syowa Station. Furthermore, we are grateful to T. Sato, H. Nishimaki, H. Yamamoto, T. Iwaki, D. Ito, S. Tasaka, A. Furusaki, M. Igarashi, T. Uemura, T. Okudaira, Y. Hasegawa, T. Yamazaki, H. Mizobuchi, M. Ikeda, K. Egawa, H. Takahashi, I. Okabayashi, E. Kishimoto for help with tethered balloon operations under severe conditions, and to A. Yukimatsu, T. Matsumoto, M. Shuto, Y. Takagi, M. Kobayashi, H. Hamamoto, K. Harada, J. Fujii, K. Harigae, and

ACPD
13, 8153–8211, 2013

Y. Ohmi for help with logistic work. Training of tethered balloon operations was conducted at the aerological observatory at Tsukuba, Japan through cooperation with Y. Shuto (JMA), and T. Kimura (aerological observatory), who also provided useful and helpful comments related to tethered balloon operation. Useful comments for balloon operations in Antarctic regions were also offered by N. Hirasawa (NIPR) and K. Sato (Univ. of Tokyo). This study was supported by "Observation project of global atmospheric change in the Antarctic" for JARE 43–47. This work was also supported by a Grant-in Aid (No. 16253001, PI: T. Yamanouchi) from the Ministry of Education, Culture, Sports, Science and Technology of Japan. The authors gratefully acknowledge the NOAA Air Resources Laboratory (ARL) for provision of the HYSPLIT transport and dispersion model and the READY website (http://www.arl.noaa.gov/ready.html) used in this publication.

References

Artaxo, P., Rabello, M. L. C., Maenhaut, W., and van Grieken, R.: Trace elements and individual particle analysis of atmospheric aerosols from the Antarctic Peninsula, Tellus, 44, 318–334, 1992.

Bodhaine, B. A.: Aerosol absorption measurements at Barrow, Mauna Loa and the South Pole, J. Geophys. Res., 100, 8967–8975, 1995.

Draxler, R. R. and Rolph, G. D.: HYSPLIT (HYbrid Single-Particle Lagrangian Integrated Trajectory) Model access via NOAA ARL READY Website available at: http://ready.arl.noaa.gov/HYSPLI~T.php, NOAA Air Resources Laboratory, Silver Spring, MD, USA, 2013.

Elsässer, C., Wagenbach, D., Weller, R., Aueri, M., Wallner, A., and Christl, M.: Continuous 25-yr aerosol records at coastal Antarctica Part 2: Variability of the radionuclides ^{7}Be, ^{10}Be and ^{210}Pb, Tellus, 63B, 920–934, 2011.

Fiebig, M., Lunder, C. R., and Stohl, A.: Tracing biomass burning aerosol from South America to Troll Research Station, Antarctica, Geophys. Res. Lett., 36, L14815, doi:10.1029/2009GL038531, 2009.

Hara, K., Kikuchi, T., Furuya, K., Hayashi, M., and Fujii, Y.: Characterization of Antarctic aerosol particles using laser microprobe mass spectrometry, Environ. Sci. Technol., 30, 385–391, 1995.

ACPD
13, 8153–8211, 2013

Hara, K., Osada, K., Hayashi, M., Matsunaga, K., Shibata, T., Iwasaka, Y., and Furuya, K.: Fractionation of inorganic nitrates in winter Arctic troposphere – coarse aerosol particles containing inorganic nitrates , J. Geophys. Res., 104, 23671–23679, 1999.

Hara, K., Osada, K., Nishita, C., Yamagata, S., Yamanocuhi, T., Herber, A., Matsunaga, K., Iwasaka, Y., Nagatani, M., and Nakada, H.: Vertical variations of sea-salt modification in the boundary layer of spring Arctic during the ASTAR 2000 campaign, Tellus, 54, 361–376, 2002.

Hara, K., Osada, K., Kido, M., Hayashi, M., Matsunaga, K., Iwasaka, Y., Yamanouchi, T., Hashida, G., and Fukatsu, T.: Chemistry of sea-salt particles and inorganic halogen species in Antarctic regions: compositional differences between coastal and inland stations, J. Geophys. Res., 109, D20208, doi:10.1029/2004JD004713, 2004.

Hara, K., Osada, K., Kido, M., Matsunaga, K., Iwasaka, Y., and Hashida, G.: Seasonal variations of sea-salt constituents and sea-salt modification at Syowa Station, Antarctica, Tellus B, 57, 230–246, 2005.

Hara, K., Iwasaka, Y., Wada, M., Ihara, T., Shiba, H., Osada, K., and Yamanouchi, T.: Aerosol constituents and their spatial distribution in the free troposphere of coastal Antarctic regions, J. Geophys. Res., 111, D15216, doi:10.1029/2005JD006591, 2006.

Hara, K., Osada, K., Yabuki, M., Hashida, G., Yamanouchi, T., Hayashi, M., Shiobara, M., Nishita-Hara, C., and Wada, M.: Haze episodes at Syowa Station, coastal Antarctica: where did they come from?, J. Geophys. Res., 115, D14205, doi:10.1029/2009JD012582, 2010a.

Hara, K., Osada, K., Yabuki, M., Hayashi, M., Yamanouchi, T., Shiobara, M., and Wada, M.: Black carbon at the coastal Antarctic station (Syowa): seasonal variation and Transport processes, Antarctic Record, 54, 562–592, 2010b (in Japanese with English abstract).

Hara, K., Osada, K., Nishita-Hara, C., Yabuki, M., Hayashi, M., Yamanouchi, T., Wada, M., and Shiobara, M.: Seasonal features of ultrafine particle volatility in the coastal Antarctic troposphere, Atmos. Chem. Phys., 11, 9803–9812, doi:10.5194/acp-11-9803-2011, 2011a.

Hara, K., Osada, K., Nishita-Hara, C., and Yamanouchi, T.: Seasonal variations and vertical features of aerosol particles in the Antarctic troposphere, Atmos. Chem. Phys., 11, 5471–5484, doi:10.5194/acp-11-5471-2011, 2011b.

Hara, K., Osada, K., Yabuki, M., and Yamanouchi, T.: Seasonal variation of fractionated sea-salt particles on the Antarctic coast, Geophys. Res. Lett., 39, L18801, doi:10.1029/2012GL052761, 2012.

ACPD
13, 8153–8211, 2013

Hayashi, M.: Size distribution of aerosol in the stratosphere and troposphere observed with air-borne optical particle counter, Earozoru Kenkyu, 16, 118–124, 2001 (in Japanese).
Hayashi, M., Osada, K., Hara, K., Yabuki, M., Kobayashi, H., Ihara, S., Wada, M., Yamanouchi, T., Hashida, G., and Shiobara, M.: Monitoring of aerosol concentration at Syowa Station, Antarctic Records, 54, 474–486, 2010 (in Japanese with English abstract).
Iizuka, Y., Hondoh, T., and Fujii, Y.: Na_2SO_4 and $MgSO_4$ salts during the Holocene period derived by high-resolution depth analysis of a Dome Fuji ice core, J. Glaciol., 52, 58–64, 2006.
Iizuka, Y., Tsuchimoto, A., Hoshina, Y., Sakurai, T., Hansson, M., Karlin, T., Fujita, K., Nakazawa, F., Motoyama, H., and Fujita, S.: The rates of sea salt sulfatization in the atmosphere and surface snow of inland Antarctica, J. Geophys. Res., 117, D04308, doi:10.1029/2011JD016378, 2012.
Ito, T.: Antarctic submicron aerosols and long-range transport of pollutants, Ambio, 18, 34–41, 1989.
Ito, T., Morita, Y., and Iwasaka, Y.: Balloon observation of aerosols in the Antarctic troposphere and stratosphere, Tellus B, 38, 214–222, 1986.
Iwasaka, Y., Okada, K., and Ono, A.: Individual aerosol particles in the Antarctic upper troposphere, Mem. Natl. Inst. Polar Res. (Special Issue) , 39, 17–29, 1985.
Jourdain, B. and Legrand, M.: Seasonal variations of atmospheric dimethylsulfide, dimethylsulfoxide, sulfur dioxide, methanesulfonate, and non-sea-salt sulfate aerosols at Dumont d'Urville (coastal Antarctica) (December 1998 to July 1999), J. Geophys. Res., 106, 14391–14408, 2001.
Jourdain, B., Preunkert, S., Cerri, O., Castebrunet, H., Udisti, R., and Legrand, M.: Year-round record of size segregated aerosol composition in central Antarctica (Concordia Station): implications for the degree of fractionation of sea-salt particles, J. Geophys. Res., 113, D14308, doi:10.1029/2007JD009584, 2008.
Keene, W. C., Maring, H., Maben, J. R., Kieber, D. J., Pszenny, A. A. P., Dahl, E. E., Izaguirre, M. A., Davis, A. J., Long, M. S., Zhou, X., Smoydzin, L., and Sander, R.: Chemical and physical characteristics of nascent aerosols produced by bursting bubbles at a model air-sea interface, J. Geophys. Res., 112, D21202, doi:10.1029/2007JD008464, 2007.
Kerminen, V. M., Teinilä, K., and Hillamo, R.: Chemistry of sea-salt particles in the summer Antarctic atmosphere, Atmos. Environ., 34, 2817–2825, 2000. Kizu, N., Hayashi, M., Yamanouchi, T., Iwasaka, Y., and Watanabe, M.: Seasonal and annual variations of aerosol

ACPD
13, 8153–8211, 2013

concentrations in the troposphere and stratosphere over Syowa Station observed using a balloon-borne optical particle counter, Antarctic Record, 54, 760–778, 2010.
Koch, D. and Hansen, J.: Distant origins of Arctic black carbon: a Goddard Institute for Space Studies model experiment, J. Geophys. Res., 110, D04204, doi:10.1029/2004JD005296, 2005.
Koponen, I. K., Virkkula, A., Hillamo, R., Kerminen, V.-M., and Kulmala, M.: Number size distributions and concentrations of the continental summer aerosols in Queen Maud Land, Antarctica, J. Geophys. Res., 108, 4587, doi:10.1029/2003JD003614, 2003.
Laskin, A., Moffet, R. C., Gilles, M. K., Fast, J. D., Zaveri, R. A., Wang, B., Nigge, P., and Shutthanandan, J.: Tropospheric chemistry of internally mixed sea salt and organic particles: surprising reactivity of NaCl with weak organic acids, J. Geophys. Res., 117, D15302, doi:10.1029/2012JD017743, 2012.
Legrand, M. and Mayewski, P.: Glaciochemistry of polar ice cores: a review, Rev. Geophys., 35, 219–243, doi:10.1029/96RG03527, 1997.
Legrand, M., Sciare, J., Jourdain, B., and Genthon, C.: Subdaily variations of atmospheric dimethylsulfide, dimethylsulfoxide, methanesulfonate, and non-sea-salt sulfate aerosols in the atmospheric boundary layer at Dumont d'Urville (coastal Antarctica) during summer, J. Geophys. Res., 106, 14409–14422, 2001.
Li, F., Ginoux, P., and Ramaswamy, V.: Transport of Patagonian dust to Antarctica, J. Geophys. Res., 115, D18217, doi:10.1029/2009JD012356, 2010.
Mamane, Y. and Gottlieb, J.: Nitrate formation on sea-salt and mineral particles – a single particle approach, Atmos. Environ., 26, 1763–1769, 1992.
Minikin, A., Legrand, M., Hall, J., Wagenbach, D., Kleefeld, C., Wolff, E., Pasteur, E., and Ducroz, F.: Sulfur-containing species (sulfate and methanesulfonate) in coastal Antarctic aerosol and precipitation, J. Geophys. Res., 103, 10975–10990, 1998.
Moore, J. K. and Abbott, M. R.: Surface chlorophyll concentrations in relation to the Antarctic Polar Front: seasonal and spatial patterns from satellite observations, J. Marine Syst., 37, 69–86, 2002.
Mouri, H., Nagao, I., Okada, K., Koga, S., and Tanaka, H.: Individual-particle analyses of coastal Antarctic aerosols, Tellus B, 51, 603–611, 1999.
Ohno, H., Igarashi, M., and Hondoh, T.: Salt inclusions in polar ice core: Location and chemical form of water-soluble impurities, Earth Planet. Sc. Lett., 232, 171–178, 2005.

ACPD
13, 8153–8211, 2013

Okada, K., Wu, P. M., Tanaka, T., and Hotta, M., A light balloon-borne sampler collecting stratospheric aerosol particles for electron microscopy, J. Meteorol. Soc. Jpn., 75, 753–760, 1997.
Okada, K., Ikegami, M., Zaizen, Y., Makino, Y., Jensen, J. B., and Gras, J. L.: The mixture state of individual aerosol particles in the 1997 Indonesian haze episode, J. Aerosol Sci., 32, 1269–1279, 2001.
Okada, K., Ikegami, M., Zaizen, Y., Tsutsumi, Y., Makino, Y., Jensen, J. B., and Gras, J. L.: Submicrometer sulfur-rich particles in the middle troposphere: aircraft observations from Australia to Japan, Atmos. Res., 88, 185–198, 2008.
Osada, K., Hayashi, M., Ui, H., and Iwasaka, Y.: Ionic constituents in aerosol particles at Syowa Station, east Antarctica, during 1996, Polar Meteorol. Glaciol., 12, 49–57, 1998.
Osada, K., Hara, K., Wada, M., Yamanouchi, T., and Matsunaga, K.: Vertical distribution of atmospheric aerosol particles over Syowa Station, east Antarctica: airborne observations from spring to summer in 2004, Polar Meteorol. Glaciol., 20, 16–27, 2006.
Piel, C., Weller, R., Huke, M., and Wagenbach, D.: Atmospheric methane sulfonate and non-sea-salt sulfate records at the European Project for Ice Coring in Antarctica (EPICA) deep-drilling site in Dronning Maud Land, Antarctica, J. Geophys. Res., 111, D03304, doi:10.1029/2005JD006213, 2006.
Pereira, K. C. D., Evangelista, H., Pereira, E. B., Simoes, J. C., Johnson, E., and Melo, L. R.: Transport of crustal microparticles from Chilean Patagonia to the Antarctic Peninsula by SEM-EDS analysis, Tellus B, 56, 262–275 doi:10.1111/j.1600-0889.2004.00105.x, 2004.
Preunkert, S., Jourdain, B., Legrand, M., Udisti, R., Becagli, S., and Cerri, O.: Seasonality of sulfur species (dimethylsulfide, sulfate, and methanesulfonate) in Antarctica: inland versus coastal regions, J. Geophys. Res., 113, D15302, doi:10.1029/2008JD009937, 2008.
Rankin, A. M. and Wolff, E. W.: Aerosol profiling using a tethered balloon in coastal Antarctica, J. Atmos. Ocean. Tech., 19, 1978–1985, 2002.
Rankin, A. M. and Wolff, E. W.: A year-long record of size-segregated aerosol composition at Halley, Antarctica, J. Geophys. Res., 108, 4775, doi:10.1029/2003JD003993, 2003.
Rankin, A. M., Auld, V., and Wolff, E. W.: Frost flowers as a source of fractionated sea salt aerosol in the polar regions, Geophys. Res. Lett., 27, 3469–3472, doi:10.1029/2000GL011771, 2000.
Rankin, A. M., Wolff, E. W., and Martin, S.: Frost flowers: Implications for tropospheric chemistry and ice core interpretation, J. Geophys. Res., 107, 4683, doi:10.1029/2002JD002492, 2002.

ACPD
13, 8153–8211, 2013

Read, K. A., Lewis, A. C., Bauguitte, S., Rankin, A. M., Salmon, R. A., Wolff, E. W., Saiz-Lopez, A., Bloss, W. J., Heard, D. E., Lee, J. D., and Plane, J. M. C.: DMS and MSA measurements in the Antarctic Boundary Layer: impact of BrO on MSA production, Atmos. Chem. Phys., 8, 2985–2997, doi:10.5194/acp-8-2985-2008, 2008.

Sato, K. and Hirasawa, N.: Statistics of Antarctic surface meteorology based on hourly data in 1957–2007 at Syowa Station, Polar Sci., 1, 1–15, 2007.

Savoie, D. L., Prospero, J. M., Larsen, R. J., and Saltzman, E. S.: Nitrogen and sulfur species in aerosols at Mawson, Antarctica, and their relationship to natural radionuclides, J. Atmos. Chem., 14, 181–204, 1992.

Savoie, D. L., Prospero, J. M., Larsen, R. J., Huang, F., Izaguirre, M. A., Huang, T., Snowdon, T. H., Custals, L., and Sanderson, C. G.: Nitrogen and sulfur species in Antarctic aerosols at Mawson, Palmer Station, and Marsh (King George Island), J. Atmos. Chem., 17, 95–122, 1993.

Shaw, G.: Bio-controlled thermostasis involving the sulfur cycles, Climatic Change, 5, 297–303, 1983.

Shaw, G. E.: Antarctic aerosols: a review, Rev. Geophys., 26, 89–112, doi:10.1029/RG026i001p00089, 1988.

Stohl, A. and Sodemann, H.: Characteristics of atmospheric transport into the Antarctic troposphere, J. Geophys. Res., 115, D02305, doi:10.1029/2009JD012536, 2010.

Suzuki, K., Yamanouchi, T., Hirasawa, N., and Yasunari, T.: Seasonal variations of air transport in the Antarctic and atmospheric circulation in 1997, Polar Meteorol. Glaciol., 18, 96–113, 2004.

Teinilä, K., Kerminen, V.-M., and Hillamo, R.: A study of size-segregated aerosol chemistry in the Antarctic atmosphere, J. Geophys. Res., 105, 3893–3904, doi:10.1029/1999JD901033, 2000.

Udisti, R., Dayan, U., Becagli, S., Busetto, M., Frosini, D., Legrand, M., Lucarelli, F., Preunkert, S., Severi, M., Traversi, R., and Vitale, V.: Sea spray aerosol in central Antarctica, Present atmospheric behaviour and implications for paleoclimatic reconstructions, Atmos. Environ., 52, 109–120, 2012.

von Glasow, R. and Sander, R.: Variation of sea-salt aerosol pH with relative humidity, Geophys. Res. Lett., 28, 247–250, 2001.

ACPD
13, 8153–8211, 2013

Wada, M., Ihara, T., and Shiba, H.: Aerological and aerosol observations in the lower atmosphere using aircraft by the 41st Japanese Antarctic Research Expedition, 2000–2001, Antarct. Record, 45, 257–278, 2001 (in Japanese with English abstract).
Wagenbach, D., Ducroz, F., Mulvaney, R., Keck, L., Minikin, A., Legrand, M. J., Hall, S., and Wolff, E. W.: Sea-salt aerosol in coastal Antarctic regions, J. Geophys. Res., 103, 10961–10974, 1998.
Weller, R. and Wagenbach, D.: Year-round chemical aerosol records in continental Antarctica obtained by automatic samplings, Tellus B, 59, 755–765, 2007.
Weller, R., Wöltjen, J., Piel, C., Resenberg, R., Wagenbach, D., König-Langlo, G., Kriews, M.: Seasonal variability of crustal and marine trace elements in the aerosol at Neumayer Station, Antarctica, Tellus B, 60, 742–752, doi:10.1111/j.1600-0889.2008.00372.x, 2008
Weller, R., Minikin, A., Wagenbach, D., and Dreiling, V.: Characterization of the inter-annual, seasonal, and diurnal variations of condensation particle concentrations at Neumayer, Antarctica, Atmos. Chem. Phys., 11, 13243–13257, doi:10.5194/acp-11-13243-2011, 2011.
Wilson, T. R.: Salinity and the major elements of sea-water, in: Chemical Oceanography, edited by: Riley, J. P. and Skirrow, G., Academic, San Diego, Calif., 365–413, 1975.
Wolff, E. W., Fischer, H., Fundel, F., Ruth, U., Twarloh, B., Littot, G. C., Mulvaney, R., Röthlisberger, R., de Angelis, M., Boutron, C. F., Hansson, M., Jonsell, U., Hutterli, M. A., Lambert, F., Kaufmann, P., Stauffer, B., Stocker, T. F., Steffensen, J. P., Bigler, M., Siggaard-Andersen, M. L., Udisti, R., Becagli, S., Castellano, E., Severi, M., Wagenbach, D., Barbante, C., Gabrielli, P., and Gaspari, V.: Southern Ocean sea-ice extent, productivity and iron flux over the past eight glacial cycles, Nature, 440, 491–496, doi:10.1038/nature04614, 2006.
Wouters, L., Artaxo, P., and van Grieken, R.: Laser microprobe mass analysis of individual antarctic aerosol particles, Int. J. Environ. An. Ch., 38, 427–438, 1990.
Yamanouchi, T., Wada, M., Fukatsu, T., Hayashi, M., Osada, K., Nagatani, M., Nakata, A., and Iwasaka, Y.: Airborne observation of water vapor and aerosols along Mizuho route, Antarctica, Polar Meteorol. Glaciol., 13, 22–37, 1999.
Yamato, M., Iwasaka, Y., Ono, A., and Yoshida, M.: On the sulfate particles in the submicron size range collected at Mizuho station and in east Queen Maud Land, Antarctica, Polar Meteorol. Glaciol. , 1, 82– 90, 1987.

ACPD
13, 8153–8211, 2013

Yamazaki, K., Okada, K., and Iwasaka, Y.: Where do aerosol particles in the Antarctic upper Troposphere come from? – a Case Study in January 1983, J. Meteor. Soc. Japan, 67, 889–906, 1989.

ACPD
13, 8153–8211, 2013

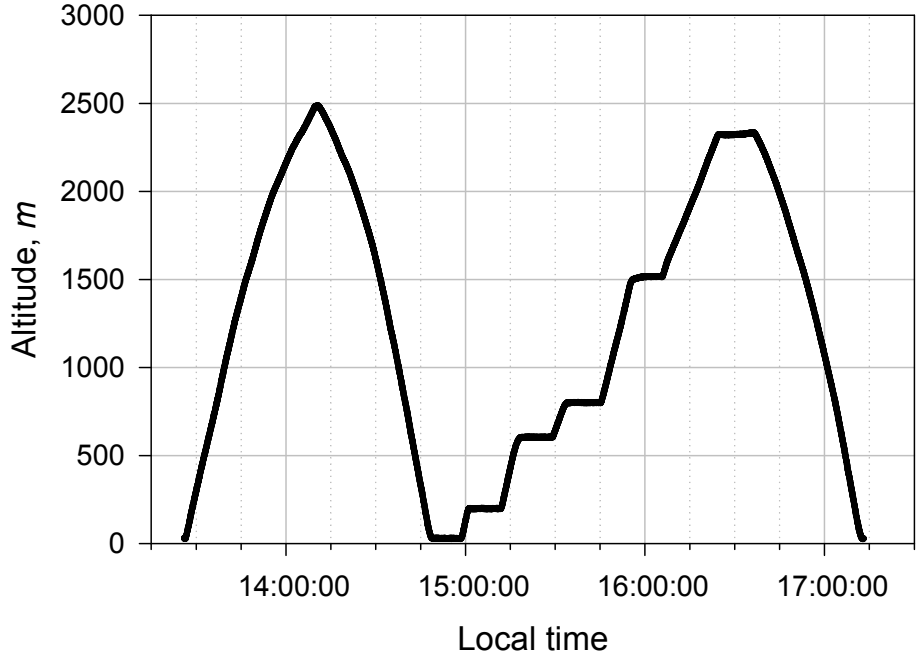

Fig. 1. Typical example of balloon trajectory (14 March 2005).

ACPD
13, 8153–8211, 2013

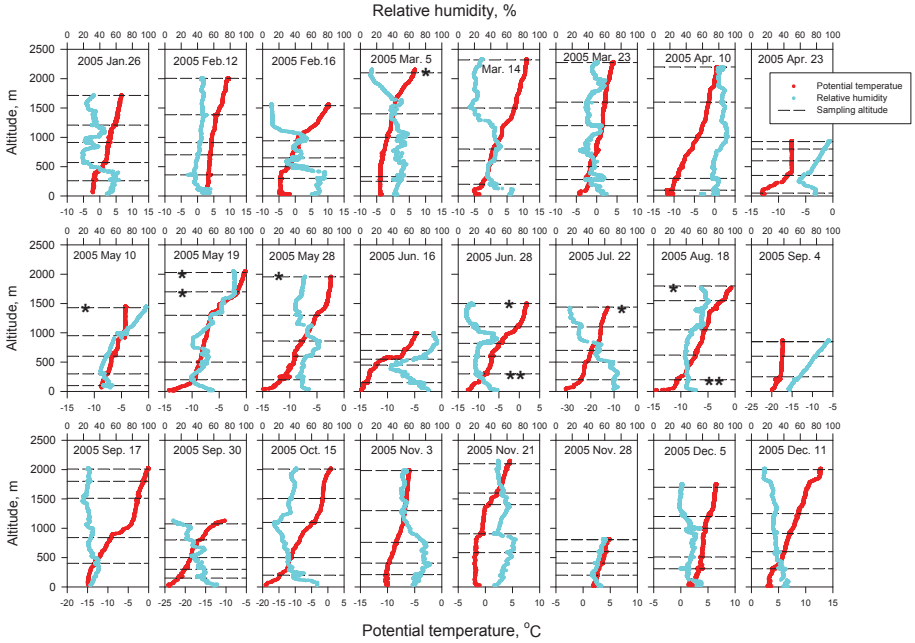

Fig. 2. Vertical profiles of potential temperature and relative humidity during the second flight. Red and blue lines respectively denote potential temperature and relative humidity. Dashed lines represent altitudes of aerosol sampling. Single and double asterisk marks respectively show “sampling failed by trouble of radio communication” and “sample disabled by damage to thin film”.

ACPD
13, 8153–8211, 2013

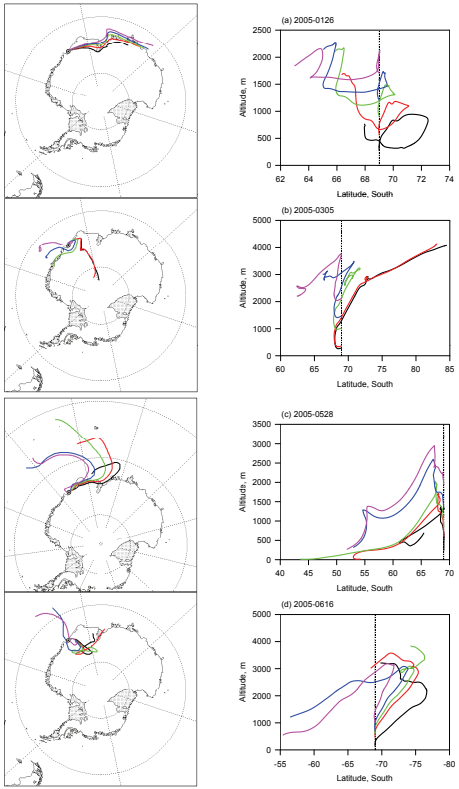

Fig. 3. Typical 5-day backward trajectories: **(a)** on 26 January, **(b)** 5 March, **(c)** 28 May, and **(d)** 16 June. Dashed lines in right panels show latitude of Syowa Station.

ACPD
13, 8153–8211, 2013

Tethered balloon-borne aerosol measurements

K. Hara et al.

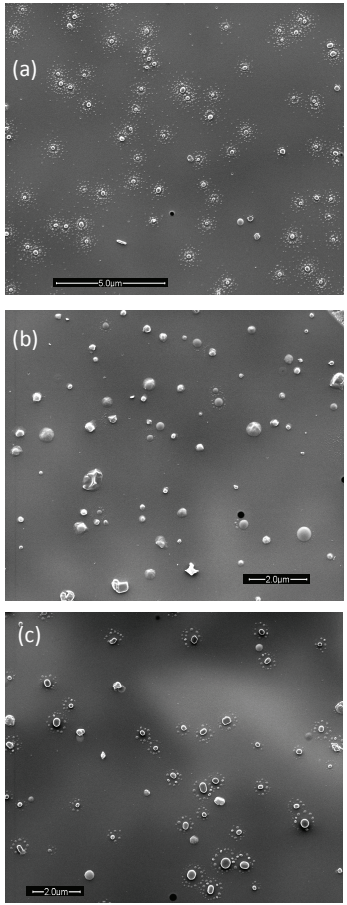

Fig. 4. Typical SEM images of aerosol particles collected **(a)** at 1245 m on 11 December, **(b)** at 498 m on 22 July, and **(c)** at 145 m on 16 June.

ACPD
13, 8153–8211, 2013

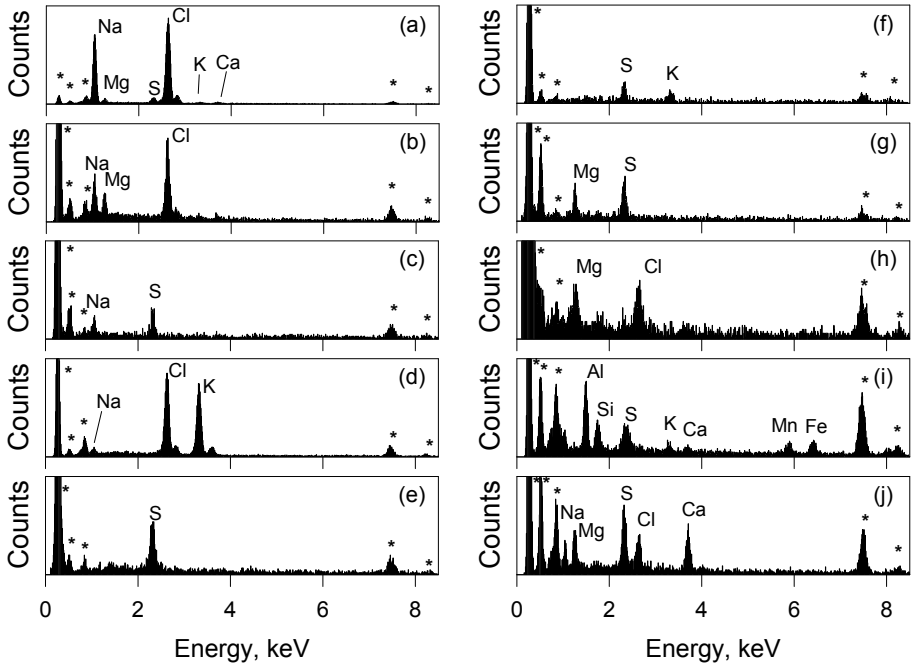

Fig. 5. Typical EDX spectra of aerosol particles collected over Syowa Station. Asterisks denote background peaks from the sample substrate. Aerosol particles were sampled **(a)** at 100 m on 10 April in fine mode, **(b)** at 200 m on 22 July in coarse mode, **(c)** at 310 m on 5 December in fine mode, **(d)** at 600 m on 10 May in coarse mode, **(e)** at 910 m on 12 February in fine mode, **(f)** at 850 m on 4 September in fine mode, **(g)** at 310 m on 11 December in fine mode, **(h)** at 1100 m on 15 October in coarse mode, **(i)** at 150 m on 16 June in coarse mode, and **(j)** at 50 m on 23 April in coarse mode.

ACPD
13, 8153–8211, 2013

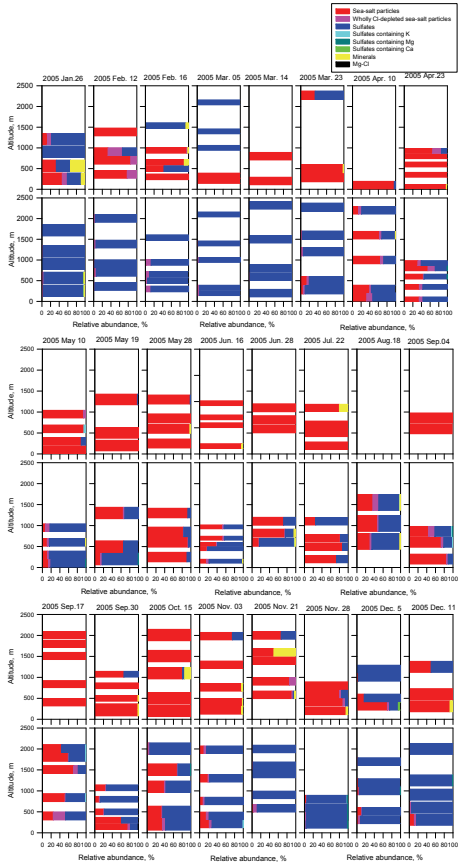

Fig. 6. Vertical features of relative abundance of each aerosol constituent in coarse and fine modes in the lower troposphere. Upper and lower panels respectively show vertical features in coarse particles and fine particles.

ACPD
13, 8153–8211, 2013

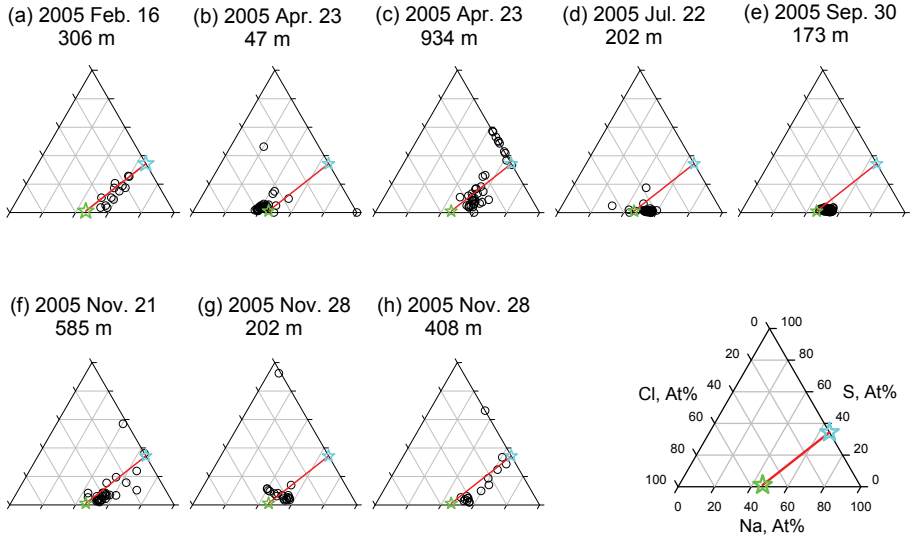

Fig. 7. Typical ternary plots of sea-salt constituents (Na, S and Cl) in coarse mode. Green and cyan star marks show atomic ratios of bulk seawater and the wholly Cl depleted sea-salt particles with sulfates. The red line represents the stoichiometric line between bulk seawater and the wholly Cl depleted sea-salt particles.

ACPD
13, 8153–8211, 2013

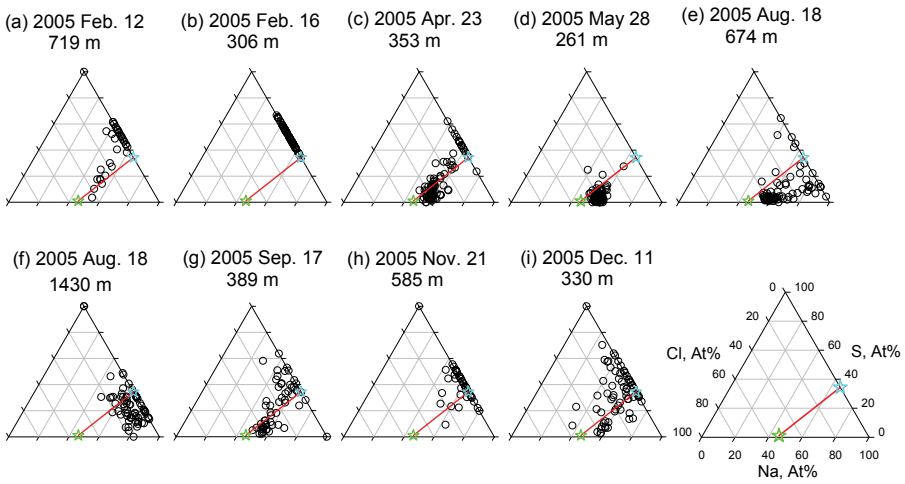

Fig. 8. Typical examples of ternary plots of sea-salt constituents (Na, S, and Cl) in fine mode. Green and cyan star marks show atomic ratios of bulk seawater and wholly Cl depleted sea-salt particles with sulfates. The red line shows the stoichiometric line between bulk seawater and the wholly Cl depleted sea-salt particles.

ACPD
13, 8153–8211, 2013

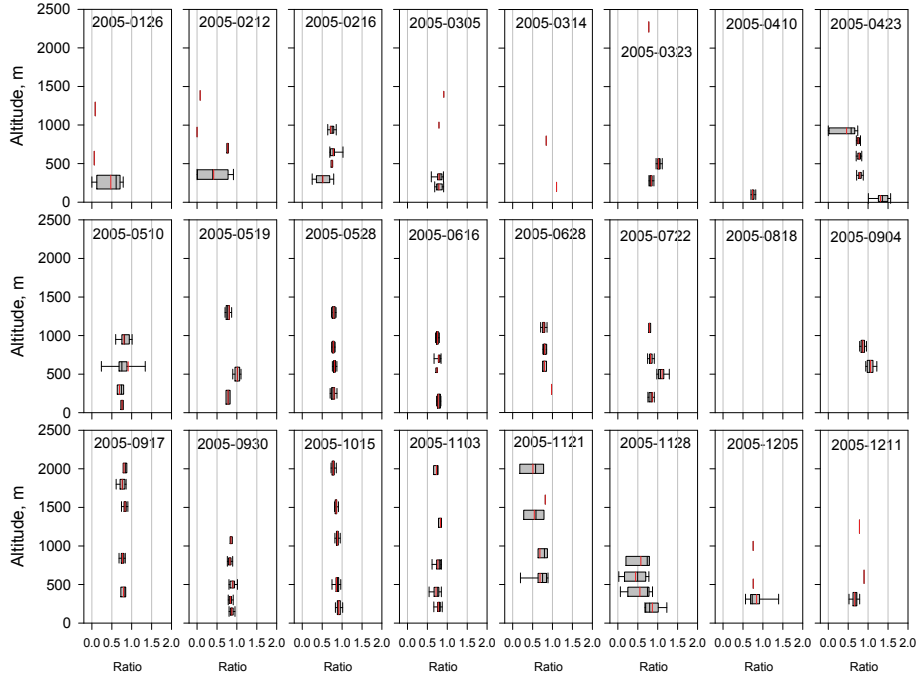

Fig. 9. Seasonal and vertical features of atomic ratios of Cl/Na in coarse mode. In box plots, the right bar, right box line, black middle box line, left box line, and left bar respectively denote values of 90 %, 75 %, 50 % (median), 25 %, and 10 %. The red line shows mean values.

ACPD
13, 8153–8211, 2013

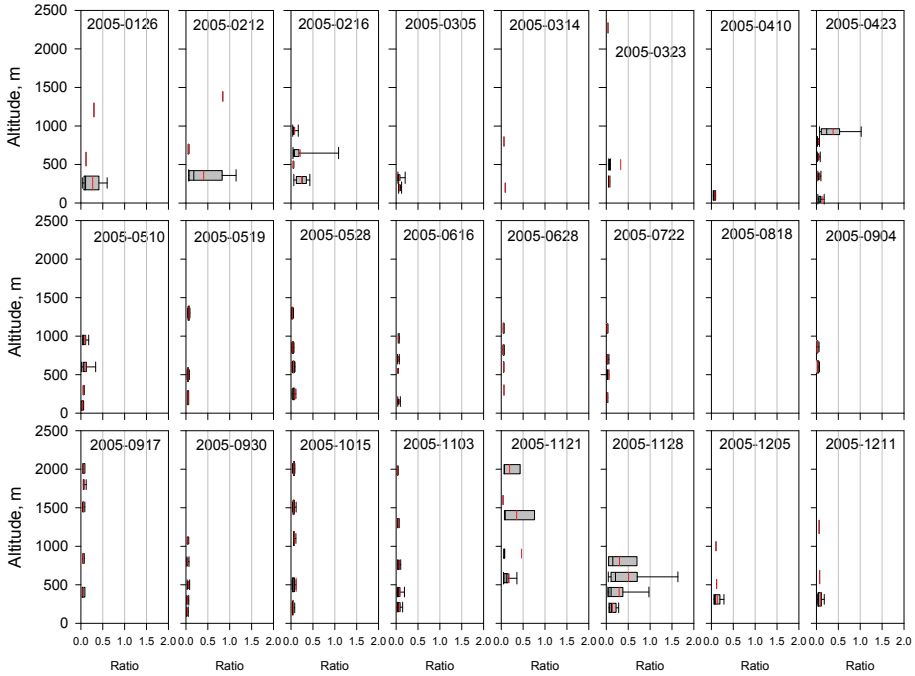

Fig. 10. Seasonal and vertical features of atomic ratios of S/Na in coarse mode. In box plots, the right bar, right box line, black middle box line, left box line, and left bar respectively denote values of 90 %, 75 %, 50 % (median), 25 %, and 10 %. The red line shows mean values.

ACPD
13, 8153–8211, 2013

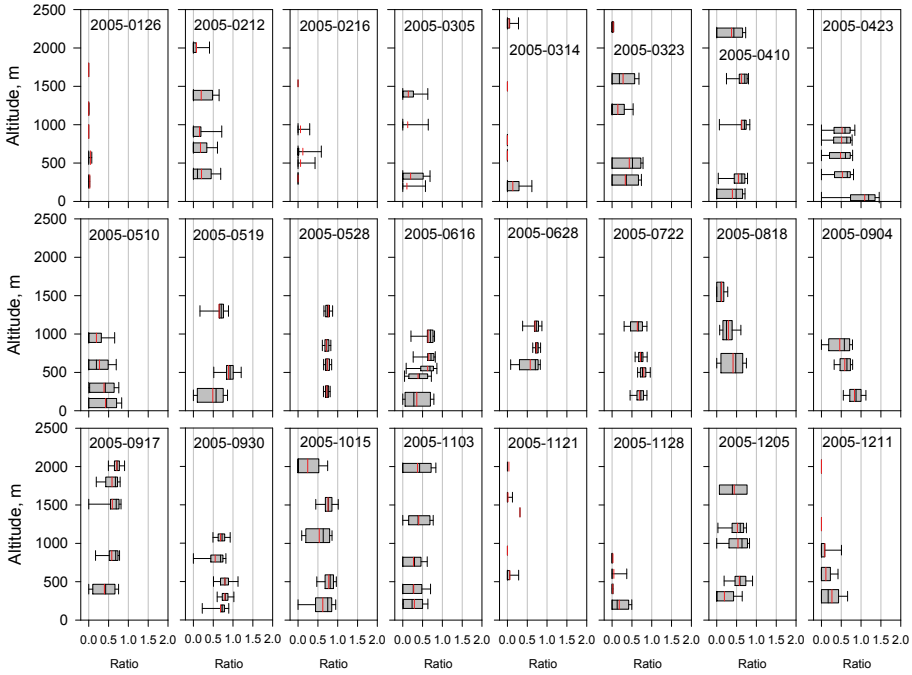

Fig. 11. Seasonal and vertical features of atomic ratios of Cl/Na in fine mode. In box plots, the right bar, right box line, black middle box line, left box line, and left bar respectively denote values of 90 %, 75 %, 50 % (median), 25 %, and 10 %. The red line shows mean values.

ACPD
13, 8153–8211, 2013

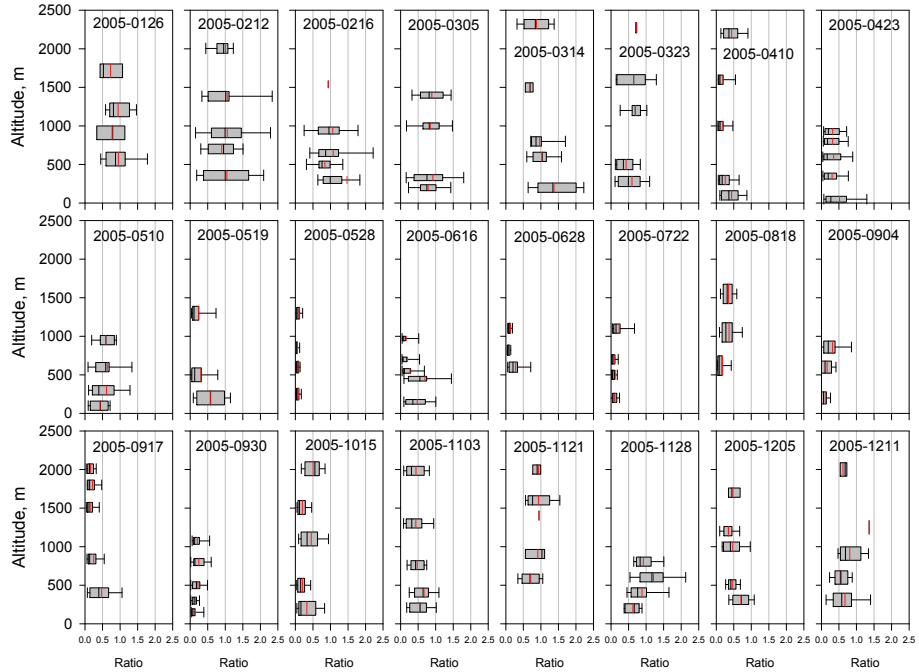

Fig. 12. Seasonal and vertical features of atomic ratios of S/Na in fine mode. In box plots, the right bar, right box line, black middle box line, left box line, and left bar respectively denote values of 90 %, 75 %, 50 % (median), 25 %, and 10 %. The red line shows mean values.

ACPD
13, 8153–8211, 2013

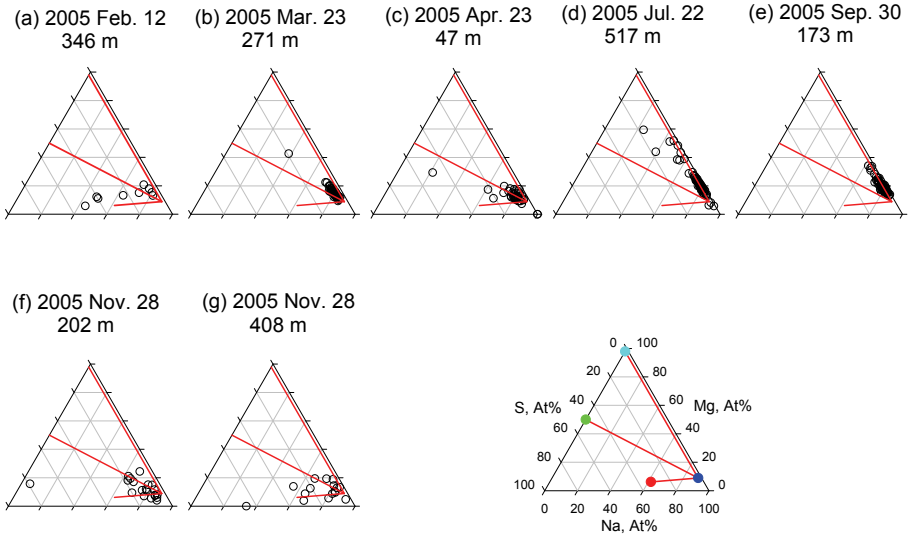

Fig. 13. Typical ternary plots of sea-salts (Na, Mg, and S) in coarse mode. Blue, red, cyan, and green circles respectively denote atomic ratios of (1) bulk seawater, (2) wholly Cl depleted sea-salt particles with sulfates, (3) $MgCl_2$, and (4) $MgSO_4$. Red lines represent stoichiometric lines among constituents.

ACPD
13, 8153–8211, 2013

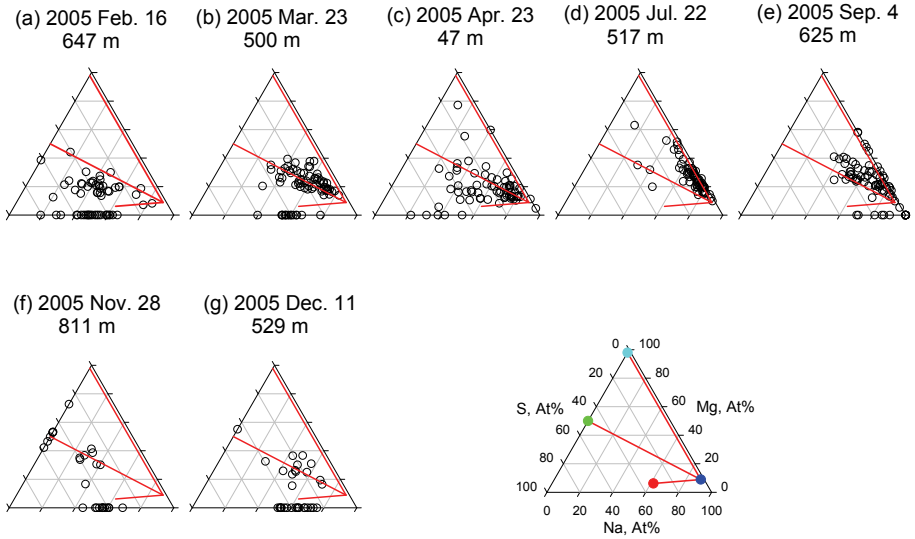

Fig. 14. Typical ternary plots of sea-salts (Na, Mg, and S) in fine mode. Blue, red, cyan, and green circles respectively denote atomic ratios of (1) bulk seawater, (2) wholly Cl depleted sea-salt particles with sulfates, (3) $MgCl_2$, and (4) $MgSO_4$. Red lines represent stoichiometric lines among constituents.

ACPD
13, 8153–8211, 2013

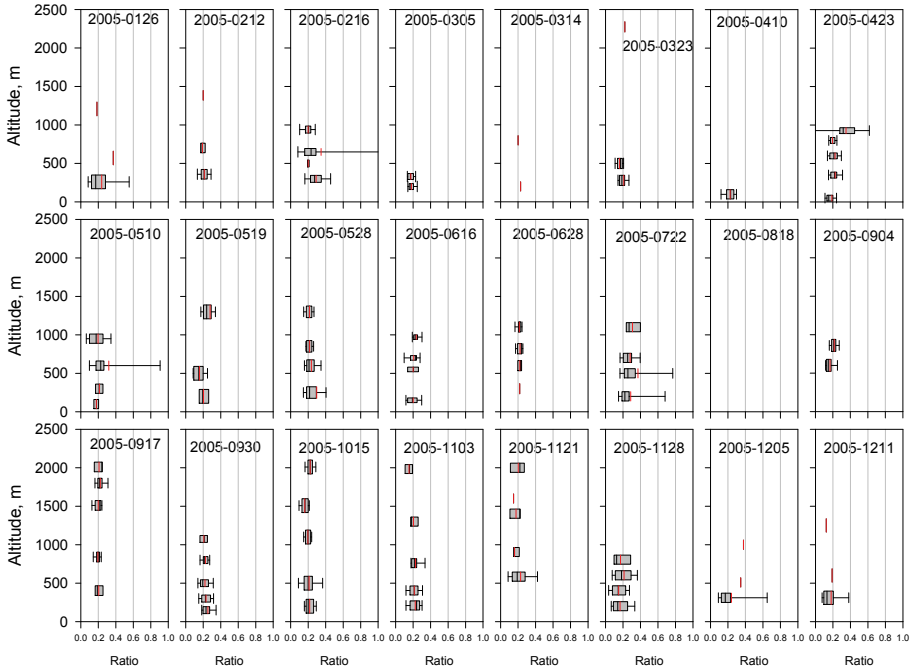

Fig. 15. Seasonal and vertical features of Mg/Na ratios in coarse modes over Syowa Station. In box plots, the right bar, right box line, black middle box line, left box line, and left bar respectively denote values of 90 %, 75 %, 50 % (median), 25 %, and 10 %. The red line shows mean values.

ACPD
13, 8153–8211, 2013

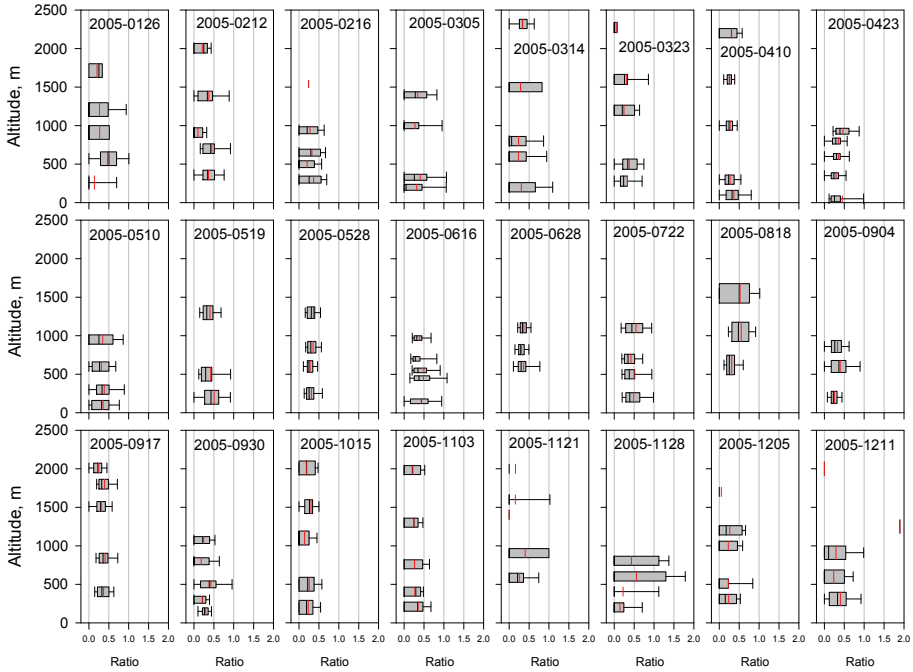

Fig. 16. Seasonal and vertical features of Mg/Na ratios in fine modes over Syowa Station. In box plots, the right bar, right box line, black middle box line, left box line, and left bar respectively denote values of 90 %, 75 %, 50 % (median), 25 %, and 10 %. The red line shows mean values.

ACPD
13, 8153–8211, 2013